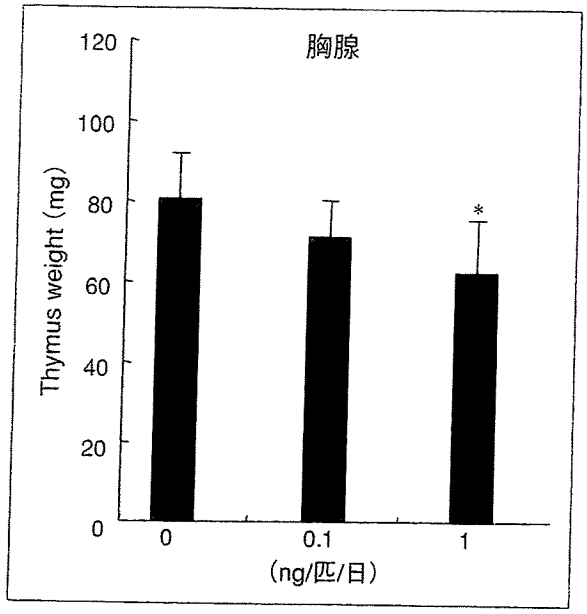

図３　新生仔期にTCDDを投与した２か月齢での胸腺の臓器重量

観察される[30]．筆者らが確立したSSのモデルマウスは舌下腺の分化異常をきたすことが知られているNFS/*sld*マウスに生後３日目においてT細胞の教育の場所である胸腺を外科的に切除することによって若齢期から高率に唾液腺，涙腺に限局する自己免疫性病変が観察される[27]．ダイオキシンによって胸腺細胞のアポトーシスが亢進するという報告に着目して，本マウスの新生仔期に胸腺を摘出する代わりにダイオキシンを投与することによって自己免疫病変が誘導されるか否かを検討した．ダイオキシンを投与されたマウスでは２か月齢において胸腺の臓器重量が対照群に比較して有意に減少していた(図３)．ダイオキシン投与により唾液腺には２か月齢より本来のモデルマウスで観察される自己免疫病変に類似した炎症性病変が観察された(図４)．病態誘導の詳細な分子機構に関しては不明であるが，新生仔期にダイオキシンに曝露されることにより胸腺の分化や成熟に異常が発生し，自己，非自己を区別する中枢性免疫寛容システムが破綻することにより，自己免疫疾患が発症したものと想定される．このことはヒトの新生児期や若齢期にダイオキシンが仮に曝露されたとすると，将来的に自己免疫疾患の発症リスクが上昇してしまう可能性を示唆している．しかし，自己免疫疾患は一つの因子で発症が決定づけられるわけではなく，遺伝因子や環境因子などが複雑に絡み合って中枢性および末梢性免疫寛容の破綻に結びついていくものと理解されているので，ダイオキシンそのものが自己免疫疾患の発症を直接的に左右しているとは言いがたい．そのレセプターであるAhRを起点とした分子シグナルの複雑さを考慮すると，ダイオキシンによる自己免疫疾患の発症に及ぼす影響には，病態に関与する免疫細胞および標的臓器細胞などへのAhRを介した分子機序に内在性のAhRリガンド，さらにホルモンなどのダイオキシンとの相互作用などさまざまな因子を考慮する必要がある．

おわりに

ダイオキシンの生体への影響に関してはその濃度が重要であることが知られている．動物実験では比較的高濃度での研究が進められているが，低濃度のダイオキシン曝露により晩発性の影響(low dose late effect)がすでに知られている．発癌，免疫異常，代謝異常など年齢という因子によって発症がある程度左右される疾患に関し

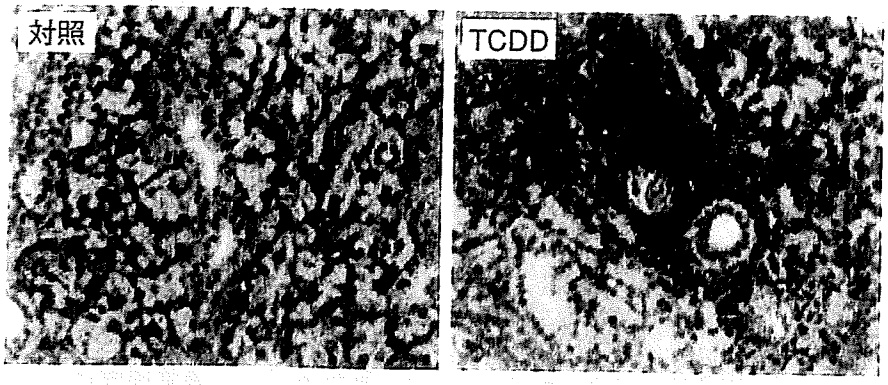

図４　新生仔期にTCDDを投与したマウスの唾液腺組織(Hematoxylin & Eosin染色)

てはダイオキシンの晩発性の影響は小さくないものと考えられる．たとえば，幼少期にダイオキシンに低濃度で曝露される環境にあれば，免疫疾患の好発年齢でより発症するリスクは高くなるのかもしれない．内分泌かく乱物質はダイオキシンだけではなく，われわれが生活する中で数多くの物質が生体内に入ってくる可能性があり，その中で内分泌かく乱物質として生体の恒常性を破綻してしまうものも現在知られているもの以外に存在する恐れもある．十年以上前に動植物のメス化とダイオキシンを代表とする内分泌かく乱物質の関係がクローズアップされてから，さまざまな角度から明らかにされてきたダイオキシンの分子メカニズムに関する研究は今後起こりうる人類に向けられた予言的な警告であると考えられる．生体システムにおいていまだ全容解明にまで至っていないさまざまな化学物質による“かく乱”の分子機構が今後明らかにされる必要がある．

文　献

1) Kerkvliet NI. Recent advances in understanding the mechanisms of TCDD immunotoxicity. Int Immunopharmacol 2001 ; 2 : 277.
2) Wormley DD, Ramesh A, Hood DB. Environmental contaminant-mixture effects on CNS development, plasticity, and behavior. Toxicol Appl Pharmacol 2004 ; 197 : 49.
3) Schecter A, Birnbaum L, Ryan JJ, et al. Dioxins : an overview. Environ Res 2006 ; 101 : 419.
4) Gehrs BC, Smialowicz RJ. Persistent suppression of delayed-type hypersensitivity in adult F344 rats after perinatal exposure to 2,3,7,8-tetrachlorodibenzo-p-dioxin. Toxicology 1999 ; 134 : 79.
5) Walker DB, Williams WC, Copeland CB, et al. Persistent suppression of contact hypersensitivity, and altered T-cell parameters in F344 rats exposed perinatally to 2,3,7,8-tetrachlorodibenzo-p-dioxin (TCDD). Toxicology 2004 ; 197 : 57.
6) Morris DL, Karras JG, Holsapple MP. Direct effects of 2,3,7,8-tetrachlorodibenzo-p-dioxin (TCDD) on responses to lipopolysaccharide (LPS) by isolated murine B-cells. Immunopharmacology 1993 ; 26 : 105.
7) Karras JG, Holsapple MP. Inhibition of calcium-dependent B cell activation by 2,3,7,8-tetrachlorodibenzo-p-dioxin. Toxicol Appl Pharmacol 1994 ; 125 : 264.
8) Quintana FJ, Basso AS, Iglesias AH, et al. Control of Treg and TH17 cell differentiation by the aryl hydrocarbon receptor. Nature 2008 ; 453 : 65.
9) Veldhoen M, Hirota K, Westendorf AM, et al. The aryl hydrocarbon receptor links TH17-cell-mediated autoimmunity to environmental toxins. Nature 2008 ; 453 : 106.
10) Laiosa MD, Wyman A, Murante FG, et al. Cell proliferation arrest within intrathymic lymphocyte progenitor cells causes thymic atrophy mediated by the aryl hydrocarbon receptor. J Immunol 2003 ; 171 : 4582.
11) Singh NP, Nagarkatti M, Nagarkatti PS. Role of dioxin response element and nuclear factor-kappaB motifs in 2,3,7,8-tetrachlorodibenzo-p-dioxin-mediated regulation of Fas and Fas ligand expression. Mol Pharmacol 2007 ; 71 : 145.
12) Prell RA, Dearstyne E, Steppan LG, et al. CTL hyporesponsiveness induced by 2,3,7,8-tetrachlorodibenzo-p-dioxin : role of cytokines and apoptosis. Toxicol Appl Pharmacol 2000 ; 166 : 214.
13) Prell RA, Oughton JA, Kerkvliet NI. Effect of 2,3,7,8-tetrachlorodibenzo-p-dioxin on anti-CD3-induced changes in T-cell subsets and cytokine production. Int J Immunopharmacol 1995 ; 17 : 951.
14) Shepherd DM, Dearstyne EA, Kerkvliet NI. The effects of TCDD on the activation of ovalbumin (OVA)-specific DO11.10 transgenic $CD4^+$ T cells in adoptively transferred mice. Toxicol Sci 2000 ; 56 : 340.
15) Dooley RK, Morris DL, Holsapple MP. Elucidation of cellular targets responsible for tetrachlorodibenzo-p-dioxin (TCDD)-induced suppression of antibody responses : II. The role of the T-lymphocyte. Immunopharmacology 1990 ; 19 : 47.
16) Luster MI, Germolec DR, Clark G, et al. Selective effects of 2,3,7,8-tetrachlorodibenzo-p-dioxin and corticosteroid on *in vitro* lymphocyte maturation. J Immunol 1990 ; 140 : 928.
17) Warren TK, Mitchell KA, Lawrence BP. Exposure

to 2,3,7,8-tetrachlorodibenzo-p-dioxin (TCDD) suppresses the humoral and cell-mediated immune responses to influenza A virus without affecting cytolytic activity in the lung. Toxicol Sci 2000 ; 56 : 123.

18) Cheon H, Woo YS, Lee JY, et al. Signaling pathway for 2,3,7,8-tetrachlorodibenzo-p-dioxin-induced TNF-α production in differentiated THP-1 human macrophages. Exp Mol Med 2007 ; 39 : 524.

19) Vorderstrasse BA, Dearstyne EA, Kerkvliet NI. Influence of 2,3,7,8-tetrachlorodibenzo-p-dioxin on the antigen-presenting activity of dendritic cells. Toxicol Sci 2003 ; 72 : 103.

20) Safe S. Molecular biology of the Ah receptor and its role in carcinogenesis. Toxicol Lett 2003 ; 120 : 1.

21) Denison MS, Heath-Pagliuso S. The Ah receptor : a regulator of the biochemical and toxicological actions of structurally diverse chemicals. Bull Environ Contam Toxicol 1998 ; 61 : 557.

22) Riddick DS, Huang Y, Harper PA, et al. 2,3,7,8-Tetrachlorodibenzo-p-dioxin versus 3-methylcholanthrene : comparative studies of Ah receptor binding, transformation, and induction of CYP1A1. J Biol Chem 1994 ; 269 : 12118.

23) Hoagland MS, Hoagland E, Swanson HI. The p53 inhibitor pifithrin-alpha is a potent agonist of aryl hydrocarbon receptor. J Pharmacol Exp Ther 2005 ; 314 : 603.

24) Vogel C, Donat S, Döhr O, et al. Effect of subchronic 2,3,7,8-tetrachlorodibenzo-p-dioxin exposure on immune system and target gene responses in mice : calculation of benchmark doses for CYP1A1 and CYP1A2 related enzyme activities. Arch Toxicol 1997 ; 71 : 372.

25) Vogel CF, Sciullo E, Li W, et al. RelB, a new partner of aryl hydrocarbon receptor-mediated transcription. Mol Endocrinol 2007 ; 21 : 2941.

26) Camacho IA, Singh N, Hegde VL, et al. Treatment of mice with 2,3,7,8-tetrachlorodibenzo-p-dioxin leads to aryl hydrocarbon receptor-dependent nuclear translocation of NF-kappaB and expression of Fas ligand in thymic stromal cells and consequent apoptosis in T cells. J Immunol 2005 ; 175 : 90.

27) Haneji N, Hamano H, Hayashi Y, et al. A new animal model for primary Sjögren's syndrome in NFS/sld mutant mice. J Immunol 1994 ; 153 : 2769.

28) Haneji N, Nakamura T, Hayashi Y, et al. Identification of alpha-fodrin as a candidate autoantigen in primary Sjögren's syndrome. Science 1997 ; 275 : 604.

29) Saegusa K, Ishimaru N, Hayashi Y, et al. Prevention and induction of autoimmune exocrinopathy is dependent on pathogenic autoantigen cleavage in murine Sjögren's syndrome. J Immunol 2002 ; 169 : 1050.

30) Fox RI. Sjögren's syndrome. Lancet 2005 ; 366 : 321.

* * *

Gene Therapy (2008), 1–5

www.nature.com/gt

SHORT COMMUNICATION

Atelocollagen-mediated local and systemic applications of myostatin-targeting siRNA increase skeletal muscle mass

N Kinouchi[1], Y Ohsawa[2], N Ishimaru[3], H Ohuchi[4], Y Sunada[2], Y Hayashi[3], Y Tanimoto[1], K Moriyama[1,5] and S Noji[4]

[1]*Department of Orthodontics and Dentofacial Orthopedics, Graduate School of Dentistry, The University of Tokushima, Tokushima, Japan;* [2]*Department of Internal Medicine, Division of Neurology, Kawasaki Medical School, Okayama, Japan;* [3]*Department of Oral Molecular Pathology, Institute of Health Bioscience, The University of Tokushima Graduate School, Tokushima, Japan and* [4]*Department of Life Systems, Institute of Technology and Science, The University of Tokushima, Tokushima, Japan*

RNA interference (RNAi) offers a novel therapeutic strategy based on the highly specific and efficient silencing of a target gene. Since it relies on small interfering RNAs (siRNAs), a major issue is the delivery of therapeutically active siRNAs into the target tissue/target cells in vivo. *For safety reasons, strategies based on vector delivery may be of only limited clinical use. The more desirable approach is to directly apply active siRNAs* in vivo. *Here, we report the effectiveness of* in vivo *siRNA delivery into skeletal muscles of normal or diseased mice through nanoparticle formation of chemically unmodified siRNAs with atelocollagen (ATCOL). ATCOL-mediated local application of siRNA targeting myostatin, a negative regulator of skeletal muscle growth, in mouse skeletal muscles or intravenously, caused a marked increase in the muscle mass within a few weeks after application. These results imply that ATCOL-mediated application of siRNAs is a powerful tool for future therapeutic use for diseases including muscular atrophy.*
Gene Therapy advance online publication, 6 March 2008; doi:10.1038/gt.2008.24

Keywords: *myostatin; RNA interference; atelocollagen; muscle; mouse; muscular dystrophy*

RNA interference (RNAi) is the process of sequence-specific, posttranscriptional gene silencing in plants and animals from flatworms to human,[1] which is mediated by ~22-nucleotide small interfering RNAs (siRNAs) generated from longer double-stranded RNA. Since it was demonstrated that siRNAs can intervene gene silencing in mammalian cells without induction of interferon synthesis or nonspecific gene suppression,[2] an increasing number of remedies utilizing highly specific siRNAs targeted against disease-causing or disease-promoting genes have been developed.[3] Effective delivery of active siRNAs to target organs or tissues is therefore the key to the development of RNAi as a broad therapeutic platform. For this purpose, different strategies have been used to deliver and achieve RNAi-mediated gene silencing *in vivo*;[3] for example, polymers represent a class of materials that meet the needs of a particular siRNA delivery system, condensing siRNAs into nano-sized particles taken up by cells.[4] However, some of the synthetic polymers, which have been used for delivery of nucleic acids, may trigger cell death in a variety of cell lines and thus suffer from limitations for its application in siRNA delivery *in vivo*.[4] On the other hand, atelocollagen (ATCOL), a pepsin-treated type I collagen lacking in telopeptides in N and C terminals that confer its antigenicity, has been shown to elicit an efficient delivery of chemically unmodified siRNAs to metastatic tumors *in vivo*.[5–7] In this study, we sought to examine the effectiveness of siRNA-ATCOL therapy for a nontumorous systemic disease, targeted against myostatin (growth/differentiation factor 8, GDF8), a negative regulator of skeletal muscle growth.[8]

Skeletal muscles are the crucial morphofunctional organs, and their atrophy causes severe conditions for life such as muscular dystrophies. Duchenne muscular dystrophy (DMD), for instance, is a severe muscle wasting disorder affecting 1 out of 3500 male birth.[9] There is currently no effective treatment, but gene therapy approaches are offering viable avenues for treatment development.[10] As one of therapeutic approaches, inhibition of myostatin by using anti-myostatin-blocking antibodies has been employed to increase muscle mass.[11] However, generating antibodies against recombinant target proteins is time consuming and requires a lot of efforts. Recently, we demonstrated that inhibition of myostatin by overexpression of the myostatin prodomain[12] prevented muscular atrophy and

Correspondence: Professor S Noji or Dr H Ohuchi, Department of Life Systems, Institute of Technology and Science, The University of Tokushima, 2-1 Minami-Jyosanjima-cho, Tokushima 770-8506, Japan.
E-mails: noji@bio.tokushima-u.ac.jp or hohuchi@bio.tokushima-u.ac.jp
[5]Current address: Department of Maxillofacial Orthognathics, Graduate School, Tokyo Medical and Dental University, Tokyo, Japan.
Received 10 October 2007; revised 26 November 2007; accepted 23 January 2008

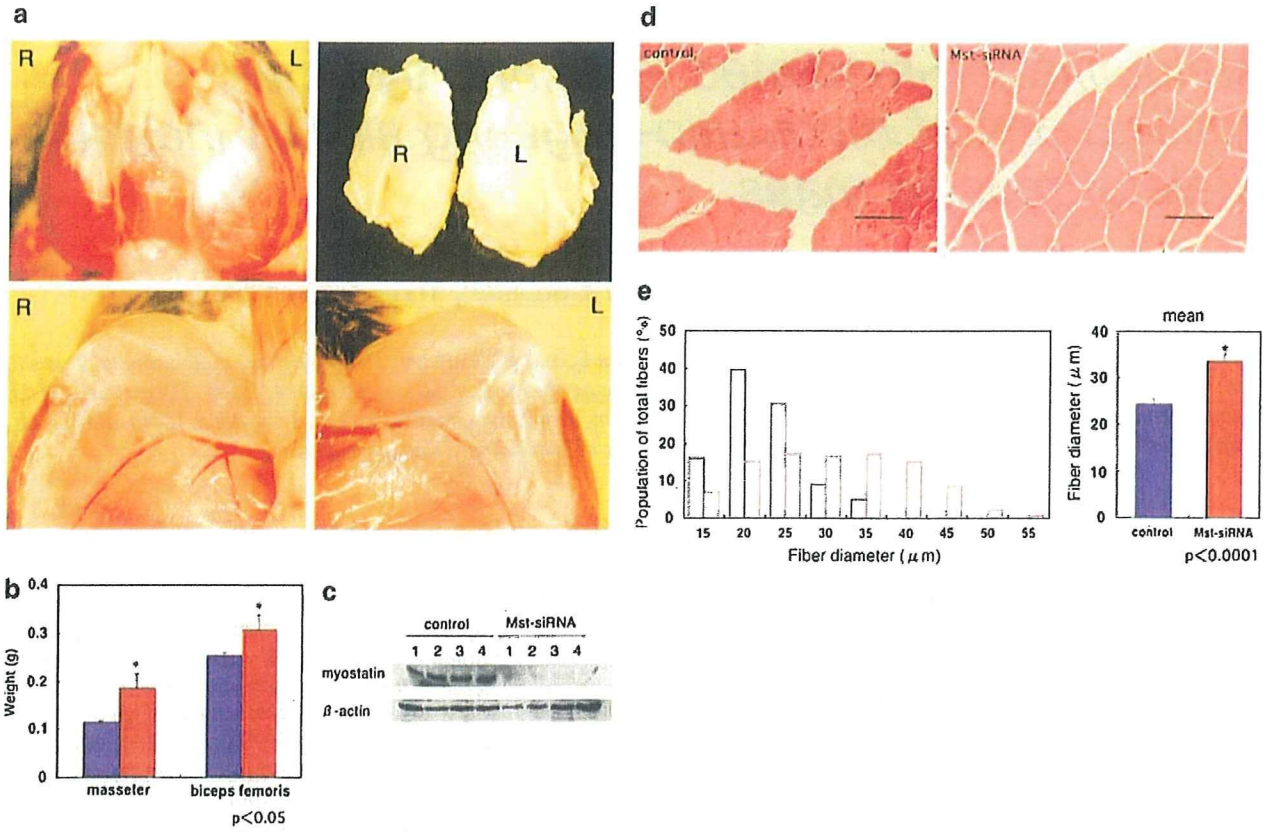

Figure 1 Local administration of the Mst-siRNA/atelocollagen (ATCOL) complex increases skeletal muscle mass and fiber size in wild-type mice through inhibition of myostatin expression. For the experiments depicted in (a–e) Mst-siRNAs (final concentration, 10 μM) were mixed with ATCOL (final concentration for local administration, 0.5%.[5]) (AteloGene, Kohken, Tokyo, Japan) according to the manufacturer's instructions. After anesthesia of mice (20-week-old male C57BL/6) by Nembutal (25 mg/kg, i.p.), the Mst-siRNA/ATCOL complex was injected into the masseter and biceps femoris muscles on the left side. As a control, scrambled siRNA/ATCOL complex was injected into the contralateral (right) muscles. After 2 weeks, the muscles on both sides were harvested and processed for analysis. (**a**) Photographs of muscles. Increased muscle mass were observed in the Mst-siRNA/ATCOL-treated (L) masseter (upper panels) and biceps femoris (lower panels), but not in the contralateral muscles (R). (**b**) Muscle weight. Mst-siRNA/ATCOL-treated muscles had an increased weight significantly compared to those with control siRNA/ATCOL (masseter, 0.185 ± 0.041 versus 0.115 ± 0.019 g; biceps, 0.307 ± 0.040 versus 0.232 ± 0.039 g; $n = 4$; $P < 0.05$). Student's *t*-test was used for determining statistical significance. Graphical representation of data uses the following convention: mean ± s.d.; treated muscles or mice in red; control muscles or mice in blue. (**c**) Western blot analysis of myostatin (52 kDa) in the control and Mst-siRNA/ATCOL-treated masseter muscles, assessed at 2 weeks after single injection. Total 80 μg of masseter muscle homogenates were resolved by sodium dodecyl sulfate–polyacrylamide gel electrophoresis and then transferred onto polyvinylidene difluoride membranes for immunoblotting. After a blocking reaction (5% nonfat milk/1% bovine serum albumin in phosphate-buffered saline (PBS) and 0.05% Triton X-100), the blots were incubated for 1 h at room temperature with mouse monoclonal anti-myostatin antibody (1:500; R&D Systems, Minneapolis, MN, USA) or anti-β-actin. After incubation with a secondary antibody (1:10000; horseradish peroxidase-conjugated anti-rat antibody; Biosource International, Camarillo, CA, USA), the blots were developed using the ECL Plus kit (Amersham, Buckinghamshire, UK). We used a purified myostatin protein and proteins extracted from cells transformed with a myostatin cDNA to confirm that the bands are due to 52 kDa myostatin. (**d**) Hematoxylin and eosin staining of the control and Mst-siRNA/ATCOL-treated masseter muscle. Muscles were fixed in 4% paraformaldehyde/PBS at 4 °C overnight, dehydrated and paraffin-embedded. Serial sections (5 μm thickness) were cut at mid-belly of muscle and stained. Scale bar, 50 μm. (**e**) Distribution of myofibril sizes of the control (blue bars) and Mst-siRNA/ATCOL-treated (red bars) muscles. The right panel shows the average myofibril size (33.6 ± 1.5 versus 24.4 ± 1.1 μm; $n = 200$; $P < 0.0001$). NIH Image (NIH, USA) software was used for morphometric measurements.

normalized intracellular myostatin signaling in the model mice for limb-girdle muscular dystrophy 1C.[13] On the other hand, Magee *et al.*[14] demonstrated that downregulation of myostatin expression by transduction of a plasmid expressing a short-hairpin interfering RNA (shRNA) against myostatin using electroporation can increase local skeletal muscle mass. For safety reasons, however, strategies based on vector delivery may be of only limited clinical use. The more desirable approach is to directly apply active siRNAs *in vivo*. As one of the practical platforms for siRNA delivery, we sought to employ an ATCOL-mediated oligonucleotide delivery system to apply myostatin-targeting siRNA into muscles.

We utilized the siRNA sequences reported previously[14] (GDF8 siRNA26, 5′-AAGATGACGATTAT CACGCTA-3′, position 426–446). It has been noted that this sequence can target myostatin mRNA not only of mouse but also human, rat, rabbit, cow, macaque and baboon, based on Blast search (National Center for Biotechnology Information).[14] To confirm the silencing effect of this siRNA, we constructed a plasmid of pSilencer 2.1-U6 neo containing the target sequence and transfected the plasmid into a mouse myoblast cell line, C2C12 cells, which had been made forced to stably express myostatin. We confirmed that the RNAi construct could effectively downregulate the expression

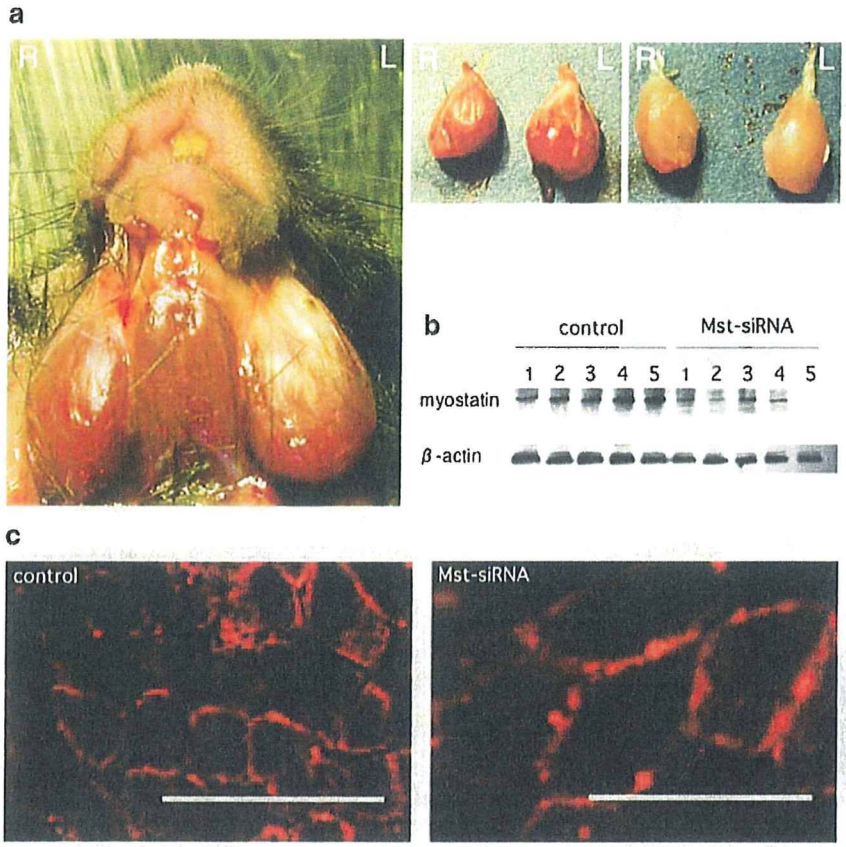

Figure 2 Mst-siRNA/atelocollagen (ATCOL) treatment improves myofibril size in *mdx* mice. (**a**) Photographs of muscles. The leftward masseter (left and middle panels) and tibial (right panel) muscles injected with the Mst-siRNA/ATCOL complex intramuscularly show a marked increased muscle mass in 20-week-old *mdx* male mice. (**b**) Western blot analysis of the control and Mst-siRNA/ATCOL-treated masseter muscles, assessed at 2 weeks after single injection. Myostatin protein levels in the muscles injected with the Mst-siRNA/ATCOL complex are markedly decreased, but not in the contralateral muscles injected with the control-siRNA/ATCOL. (**c**) Immunohistochemical analysis of the cross-sectional myofiber area of the masseter muscle, with the anti-laminin α2 antibody (4H8-2, Sigma, St Louis, MO, USA), showing increased fiber size in the Mst-siRNA/ATCOL-treated (right panel) muscle, compared to that of control (left panel). Alexafluor 594-conjugated anti-rat immunoglobulin G antibodies (A-11007, Invitrogen, Carlsbad, CA, USA) were used for immunohistochemistry. Scale bar, 100 μm.

of myostatin in the C2C12 cells[15] (Supplementary Figure S1).

We prepared the nanoparticle complex containing the GDF8 siRNA26 (10 μM) and ATCOL. Then, we injected the GDF8 siRNA26-ATCOL (Mst-siRNA/ATCOL) complex into the masseter and biceps femoris muscles of 20-week-old C57BL/6 mice. As a control, we injected control-scrambled siRNAs/ATCOL complex in the contralateral muscles. We observed gross morphology of the muscles and dissected the muscle tissues 2 weeks after injection. After injection of the Mst-siRNA/ATCOL complex, both muscles (on the left side) were enlarged, while no significant change was observed on the contralateral side (Figure 1a). We also measured the muscle weight, finding that the Mst-siRNA/ATCOL-treated muscles weighed significantly more than those on the control side (Figure 1b). The Mst-siRNA/ATCOL-treated muscles were further examined by a western blot analysis for myostatin (52 kDa), showing the decreased expression of myostatin on the treated side (Figure 1c). We quantified each result as a ratio to the internal control and statistically analyzed a difference between control (average ratio 0.90 ± 0.07) and treated (average ratio 0.44 ± 0.22) muscles. This difference is significant ($P < 0.01$, Student's t-test, $n = 4$). Histological analysis showed that the myofibril sizes of the masseter muscles treated with the Mst-siRNA/ATCOL complex were larger than those of the control (Figure 1d). Examining the sizes of 200 myofibers per group, the population of myofibril sizes indicated a shift from smaller to larger fibers in the Mst-siRNA/ATCOL-treated muscle (Figure 1e). The average myofibril size of the muscle treated with Mst-siRNA/ATCOL gained approximately 1.3 times more than that of control (Figure 1e). No obvious morphological change was observed in other tissues than the treated masseter muscles. In the meanwhile, we did not observe any general sign of ill health and deaths during the period of experiment. These results indicate that the increase of the Mst-siRNA/ATCOL-treated muscle mass is caused by their hypertrophy and that the siRNA complex gives no obvious adverse effects.

We next questioned whether this effect of hypertrophy after local injection of the Mst-siRNA/ATCOL complex observed in normal mice was relevant to dystrophin-deficient *mdx* mouse, an animal model for DMD.[16] We intramuscularly injected the same Mst-siRNA/ATCOL complex into the masseter and tibial muscles on the left side of 20-week-old *mdx* male mice. Within 2 weeks after the single injection, a dramatically increased muscle

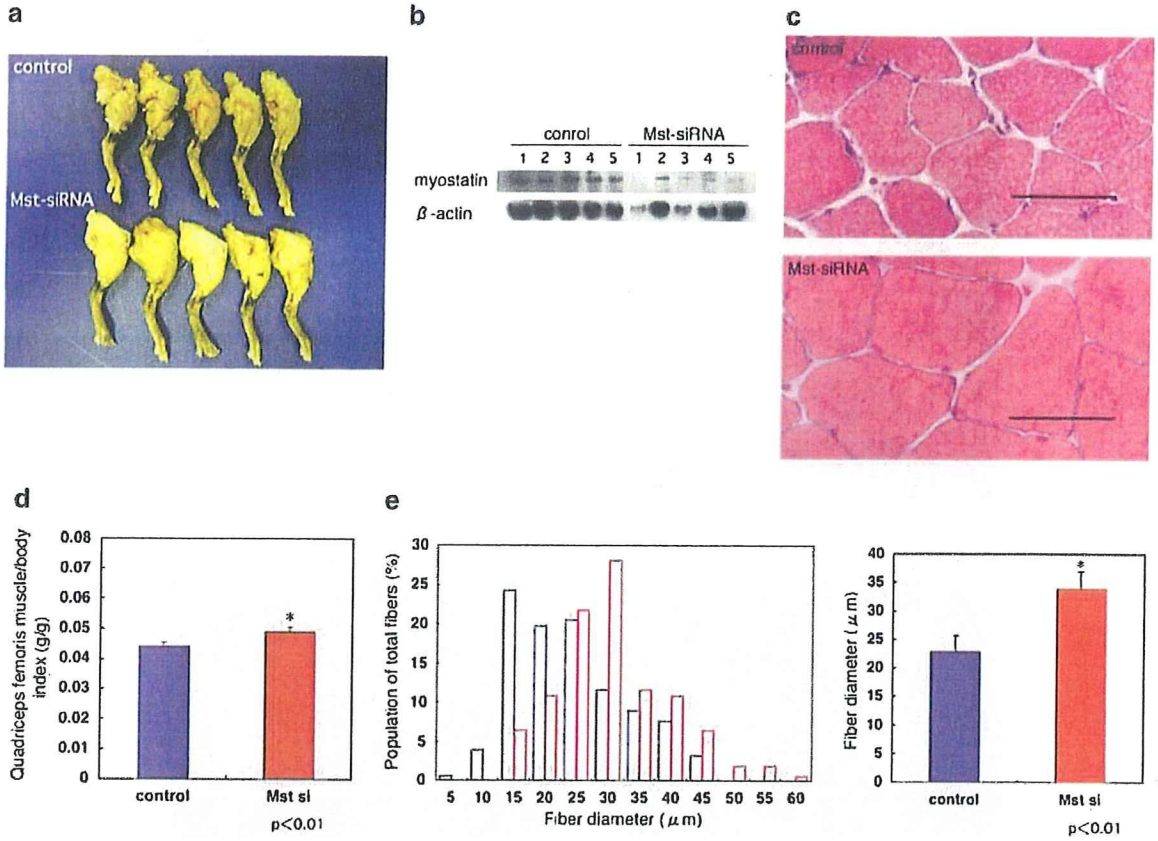

Figure 3 Systemic administration of the Mst-siRNA/atelocollagen (ATCOL) complex induces muscle enlargement in the mouse through inhibition of myostatin expression. For systemic administration, the siRNA (final concentration, 40 μM)/ATCOL (final concentration, 0.05%[6] complex, 200 μl) was introduced intravenously via orbital veins at 4, 7 and 14 days after the first application ($n=5$). As a control, control-scrambled siRNAs were injected into wild-type male mice (20 weeks, $n=5$). After 3 weeks, the quadriceps muscles on both sides were harvested and processed for analysis. (**a**) Photographs of lower limbs from control (upper panel) and Mst-siRNA/ATCOL-treated (lower panel) mice. (**b**) Western blot analysis of the control and Mst-siRNA/ATCOL-treated muscles (quadriceps femoris), assessed at 3 weeks after triple injection. (**c**) Hematoxylin and eosin staining of the control (upper panel) and Mst-siRNA/ATCOL-treated quadriceps muscle (lower panel). Scale bar, 50 μm. (**d**) Comparison of muscle weight/body weight index between the Mst-siRNA/ATCOL and control-siRNA/ATCOL-treated mice (0.048 ± 0.002 versus 0.043 ± 0.001 $n=5$; $P<0.01$). (**e**) Distribution of myofibril sizes of the control and Mst-siRNA/ATCOL-treated quadriceps muscles. The right panel shows the average myofibril size (33.92 ± 2.91 versus 22.95 ± 1.54 μm, $n=156$; $P<0.01$).

mass was observed in the Mst-siRNA/ATCOL-treated muscle (Figure 2a). Western blot analysis showed that the protein levels of myostatin in the muscles treated with the Mst-siRNA/ATCOL complex were significantly decreased (average ratio 0.55 ± 0.03), but not in the contralateral muscles treated with control siRNAs/ATCOL complex (average ratio 0.83 ± 0.01) (Figure 2b; $P<0.05$, $n=5$). Furthermore, immunohistochemical analysis on the masseter using an anti-laminin α2 antibody showed increase in the mean myofiber size of the Mst-siRNA/ATCOL-treated muscle (Figure 2c), as is the case for the wild-type (not shown). On the basis of these results, it seems that myostatin maintains satellite cells or muscle stem cells in a quiescent state. Reduced myostatin activity would lead to activation of these cells and fusion into existing fibers (Supplementary Figure S1e and f), resulting in fiber hypertrophy as proposed previously.[14]

We further examined whether systemic administration of the Mst-siRNA/ATCOL complex would have an effect on silencing the myostatin expression and lead to muscle enlargement. The Mst- or control siRNA/ATCOL complex was applied intravenously into normal mice four times in 3 weeks. Strikingly, we observed an obvious enlargement of skeletal muscles of lower limbs (Figure 3a), masseters and other muscles. Since change in the muscles of lower limbs is much larger than others, we used them for further analyses. We confirmed reduction of myostatin proteins in the muscles treated with the Mst-siRNA/ATCOL complex (average ratio 0.67 ± 0.11) (Figure 3b; $P<0.01$, $n=5$; average ratio for control 0.87 ± 0.03). We observed that the treated lower limbs are much larger than the controls, although the average body weights were 26.7 ± 0.7 and 25.8 ± 0.4 g for controls and treated mice, respectively. No increase in the body weight of the treated mouse was observed, probably because increase in the muscle weight compensated for reduction of fat accumulation.[17] To show increase in muscle weights, we used the muscle weight/body weight ratio (Figure 3d), in case the body weight exhibited variation. Significant increase in muscle fiber size (Figures 3c and e) was also observed after 3 weeks. These results indicate that siRNAs targeting against myostatin, intravenously administered with ATCOL, can specifically repress the expression of myostatin, inducing muscle hypertrophy in normal mice.

We present evidence that local and systemic applications of siRNA against myostatin coupled with ATCOL markedly stimulate muscle growth *in vivo* within a few

weeks. Local application of siRNA/ATCOL complex was shown to be effective to target the vascular endothelial growth factor gene in a xenografted tumor,[18] while ATCOL was used for systemic siRNA delivery into tumor-bearing mouse models and proved to be effective for silencing exogenous genes as luciferase and metastasis-associated genes as EZH2.[6] However, it has not been elucidated until this study whether the siRNA complex could have an effect of muscle growth on normal tissues by repression of muscle-specific genes. It has been thought that the enhanced permeability and retention (EPR) effect in tumor tissues could facilitate selective targeting of siRNA/polymer complex.[6] In spite of the significance of the EPR effect in tumor therapies, it is noticeable that normal and nontumor diseased tissues can be targets for siRNA-based drugs applied systemically. It was reported that nuclease activity to siRNA could be prevented[18] and cellular uptake of siRNAs was elevated by ATCOL.[5] Although the precise mechanisms by which ATCOL achieves these effects have not been elucidated to date, ATCOL complexed with DNA molecules was demonstrated to be efficiently transduced into mammalian cells.[19] Thus, similarly siRNA/ATCOL complexes may be transduced into cells probably by the same mechanisms as observed for DNA molecules. As a simple administration of myostatin-siRNA/ATCOL complex has a muscle growth effect, this novel method for fighting against muscle atrophy would be of considerable value for clinical applications. In tumor-bearing mice, it was reported that ATCOL could distribute siRNAs against luciferase to normal liver, lung, spleen and kidney tissues as well as bone-metastatic lesions.[6] ATCOL was also reported to display low toxicity and low immunogenicity when it is transplanted *in vivo*.[20,21] Taken together with our results, application of siRNAs with ATCOL would be promising for a therapeutic remedy against various diseases not only of muscles, but also of these organs.

Acknowledgements

We thank Drs Shin-ichiro Nishimatsu, Tsutomu Nohno, Department of Molecular Biology, Kawasaki Medical School for valuable advice. We also thank Shizuka Sasano, Division of Neurology, Kawasaki Medical School and Megumu Kita, Laboratory Animal Center, Kawasaki Medical School for their technical assistances. This work was supported by a Research Grant (14B-4) for Nervous and Mental Disorders from the Ministry of Health, Labour and Welfare; a Grant (15131301) for Research on Psychiatric and Neurological Diseases and Mental Health from the Ministry of Health, Labour and Welfare of Japan and from JSPS KAKENHI (14370212) to SN, YO and YS and by Research Project Grants (15-115B and 16-601) from Kawasaki Medical School to YO and YS.

References

1 Fire A, Xu S, Montgomery MK, Kostas SA, Driver SE, Mello CC. Potent and specific genetic interference by double-stranded RNA in *Caenorhabditis elegans*. *Nature* 1998; **391**: 806–811.
2 Elbashir SM, Harborth J, Lendeckel W, Yalcin A, Weber K, Tuschl T. Duplexes of 21-nucleotide RNAs mediate RNA interference in cultured mammalian cells. *Nature* 2001; **411**: 494–498.
3 de Fougerolles A, Vornlocher HP, Maraganore J, Lieberman J. Interfering with disease: a progress report on siRNA-based therapeutics. *Nat Rev Drug Discov* 2007; **6**: 443–453.
4 Gary DJ, Puri N, Won YY. Polymer-based siRNA delivery: perspectives on the fundamental and phenomenological distinctions from polymer-based DNA delivery. *J Control Release* 2007; **121**: 64–73.
5 Minakuchi Y, Takeshita F, Kosaka N, Sasaki H, Yamamoto Y, Kouno M *et al*. Atelocollagen-mediated synthetic small interfering RNA delivery for effective gene silencing *in vitro* and *in vivo*. *Nucleic Acids Res* 2004; **32**: e109.
6 Takeshita F, Minakuchi Y, Nagahara S, Honma K, Sasaki H, Hirai K *et al*. Efficient delivery of small interfering RNA to bone-metastatic tumors by using atelocollagen *in vivo*. *Proc Natl Acad Sci USA* 2005; **102**: 12177–12182.
7 Takeshita F, Ochiya T. Therapeutic potential of RNA interference against cancer. *Cancer Sci* 2006; **97**: 689–696.
8 McPherron AC, Lawler AM, Lee SJ. Regulation of skeletal muscle mass in mice by a new TGF-beta superfamily member. *Nature* 1997; **387**: 83–90.
9 Deconinck N, Dan B. Pathophysiology of Duchenne muscular dystrophy: current hypotheses. *Pediatr Neurol* 2007; **36**: 1–7.
10 Foster K, Foster H, Dickson JG. Gene therapy progress and prospects: Duchenne muscular dystrophy. *Gene Therapy* 2006; **13**: 1677–1685.
11 Bogdanovich S, Krag TO, Barton ER, Morris LD, Whittemore LA, Ahima RS *et al*. Functional improvement of dystrophic muscle by myostatin blockade. *Nature* 2002; **420**: 418–421.
12 Nishi M, Yasue A, Nishimatsu S, Nohno T, Yamaoka T, Itakura M *et al*. A missense mutant myostatin causes hyperplasia without hypertrophy in the mouse muscle. *Biochem Biophys Res Commun* 2002; **293**: 247–251.
13 Ohsawa Y, Hagiwara H, Nakatani M, Yasue A, Moriyama K, Murakami T *et al*. Muscular atrophy of caveolin-3-deficient mice is rescued by myostatin inhibition. *J Clin Invest* 2006; **116**: 2924–2934.
14 Magee TR, Artaza JN, Ferrini MG, Vernet D, Zuniga FI, Cantini L *et al*. Myostatin short interfering hairpin RNA gene transfer increases skeletal muscle mass. *J Gene Med* 2006; **8**: 1171–1181.
15 Artaza JN, Bhasin S, Magee TR, Reisz-Porszasz S, Shen R, Groome NP *et al*. Myostatin inhibits myogenesis and promotes adipogenesis in C3H 10T(1/2) mesenchymal multipotent cells. *Endocrinology* 2005; **146**: 3547–3557.
16 Bulfield G, Siller WG, Wight PA, Moore KJ. X chromosome-linked muscular dystrophy (mdx) in the mouse. *Proc Natl Acad Sci USA* 1984; **81**: 1189–1192.
17 McPherron AC, Lee SJ. Suppression of body fat accumulation in myostatin-deficient mice. *J Clin Invest* 2002; **109**: 595–601.
18 Takei Y, Kadomatsu K, Yuzawa Y, Matsuo S, Muramatsu T. A small interfering RNA targeting vascular endothelial growth factor as cancer therapeutics. *Cancer Res* 2004; **64**: 3365–3370.
19 Honma K, Ochiya T, Nagahara S, Sano A, Yamamoto H, Hirai K *et al*. Atelocollagen-based gene transfer in cells allows high-throughput screening of gene functions. *Biochem Biophys Res Commun* 2001; **289**: 1075–1081.
20 Ochiya T, Nagahara S, Sano A, Itoh H, Terada M. Biomaterials for gene delivery: atelocollagen-mediated controlled release of molecular medicines. *Curr Gene Ther* 2001; **1**: 31–52.
21 Sano A, Maeda M, Nagahara S, Ochiya T, Honma K, Itoh H *et al*. Atelocollagen for protein and gene delivery. *Adv Drug Deliv Rev* 2003; **55**: 1651–1677.

Supplementary Information accompanies the paper on Gene Therapy website (http://www.nature.com/gt)

ARTHRITIS & RHEUMATISM
Vol. 58, No. 2, February 2008, pp 389–400
DOI 10.1002/art.23163

Effective Treatment With Oral Administration of Rebamipide in a Mouse Model of Sjögren's Syndrome

Masayuki Kohashi,[1] Naozumi Ishimaru,[2] Rieko Arakaki,[2] and Yoshio Hayashi[2]

Objective. **To determine whether oral administration of rebamipide, a mucosal protective agent, is effective in the treatment of Sjögren's syndrome (SS) in the NFS/*sld* mouse model of the disease.**

Methods. **NFS/*sld* mice were given daily oral doses of rebamipide (0.3 mg/kg of body weight or 3 mg/kg) or vehicle alone starting from the age of 4 weeks to the age of 8 weeks. The volume of saliva and tears was monitored during and after treatment. After the final dose, histologic features of the tissues, TUNEL+ apoptotic duct cells in affected glands, T cell and cytokine function, and levels of immunoglobulin isotypes and serum autoantibodies were examined.**

Results. **The 3-mg/kg dose of rebamipide prevented the development of autoimmune lesions. The average volume of saliva in rebamipide-treated mice was significantly higher than that in control mice. We found decreased TUNEL+ apoptotic duct cells in the salivary and lacrimal glands of rebamipide-treated mice as compared with control mice. Rebamipide treatment suppressed the activation of CD4+ T cells and Th1 cytokines (interleukin-2, interferon-γ) associated with impaired NF-κB activity. Production of serum autoantibodies, IgM, and IgG1 was clearly inhibited.**

Conclusion. **Our findings demonstrate the efficacy of oral administration of rebamipide in the treatment of SS. Rebamipide represents a new therapeutic strategy for the treatment of patients with sicca symptoms caused by SS, as well as for patients with other diseases.**

Sjögren's syndrome (SS) is an autoimmune disorder characterized by lymphocytic infiltrates and destruction of the salivary and lacrimal glands, as well as systemic production of autoantibodies to the RNP particles SSA/Ro and SSB/La (1–3). Although the specificity of cytotoxic T lymphocyte function has been an important issue in studies of organ-specific autoimmune responses, the mechanisms responsible for tissue destruction in SS remain to be fully elucidated. The immune system has acquired regulatory mechanisms that preclude the reactivity of mature T cells to self antigens presented by major histocompatibility complex (MHC) molecules, while maintaining an ability to respond to non-self antigens presented by self MHC molecules (4,5). The dysregulation of T cell tolerance is considered to be responsible for many types of autoimmune diseases, and a variety of mechanisms involved in the initiation of autoimmune diseases have been proposed (6–10).

Data from our previous studies demonstrated that autoreactive CD4+ T cells play a pivotal role in the development of autoimmune exocrinopathy in the NFS/*sld* mouse model of SS (11). It is now evident that the interaction of Fas with FasL regulates a large number of pathophysiologic processes of apoptosis, including autoimmune diseases (11,12). Previous studies have also confirmed the observation that apoptotic cells in various cell types are implicated as the source of autoantigen when stimulated with different proapoptotic stimuli (13).

On the other hand, natural autoantibody appears to be primarily IgM polyreactive antibody of low affinity, which is quite different from the monospecific high-affinity IgG antibody usually associated with autoimmune disease (14). It is important to note that au-

Supported in part by the Ministry of Education, Science, Sports, and Culture of Japan (Grants-in-Aid for Scientific Research 17109016 and 17689049) and the Uehara Memorial Foundation.

[1]Masayuki Kohashi, PhD: University of Tokushima Graduate School, and Otsuka Pharmaceutical Company, Ltd., Tokushima, Japan; [2]Naozumi Ishimaru, DDS, PhD, Rieko Arakaki, PhD, Yoshio Hayashi, DDS, PhD: University of Tokushima Graduate School, Tokushima, Japan.

Address correspondence and reprint requests to Yoshio Hayashi, DDS, PhD, Department of Oral Molecular Pathology, Institute of Health Biosciences, University of Tokushima Graduate School, 3 Kuramoto-cho, Tokushima 770-8504, Japan. E-mail: hayashi@dent.tokushima-u.ac.jp.

Submitted for publication June 15, 2007; accepted in revised form October 26, 2007.

toantigens released from the intracytoplasmic environment will not, under normal conditions, stimulate the production of pathogenic IgG autoantibodies capable of causing tissue damage (14,15). During an autoimmune disease, levels of IgM autoantibodies are high (16) due to the stimulation of IgM autoantibody–producing cell lines by the release of autoantigens from target cells. IgG antibodies are the primary mediators of protective humoral immunity against pathogens, but they can also be pathogenic. Acting as cytotoxic molecules or as immune complexes, IgG autoantibodies are the principal mediators of autoimmune diseases such as idiopathic thrombocytopenia, autoimmune hemolytic anemia, and systemic lupus erythematosus, and may contribute to other autoimmune diseases, such as rheumatoid arthritis, type 1 diabetes mellitus, and multiple sclerosis (17).

Rebamipide (2-[4-chlorobenzoylamino]-3-[2(1*H*)quinolinon-4-yl]propionic acid; OPC-12759) is a mucosal protective agent used for the treatment of gastritis and gastric ulcer. It has recently been reported that rebamipide works as an antiinflammatory agent in both acute and chronic inflammation and has an inhibitory effect on proinflammatory cytokines (18). Experimental data have shown that rebamipide can prevent Dextran sulfate sodium–induced colitis in rats (19). A recent study demonstrated the protective effect of rebamipide on the intestinal barrier, namely, its ability to reinforce the epithelial barrier capacity and to decrease macromolecular transport across this barrier (20). At the same time, the study demonstrated the immunoregulatory properties of rebamipide, which is capable of regulating lymphocyte proliferation and cytokine secretion (20).

The aim of the present study was to investigate the effects of oral administration of rebamipide on various parameters of autoimmune responses and on serum levels of autoantibodies, immunoglobulins, and inflammatory cytokines in a murine model of SS. We hypothesized that in this model of SS, the immunomodulatory activity of rebamipide against autoimmune responses to tissue-specific autoantigens would be a good therapeutic approach.

MATERIALS AND METHODS

Mice and experimental design. Female mice of the NFS/N strain carrying the mutant gene *sld* (21) were reared in our specific pathogen–free mouse colony and given food and water ad libitum. Thymectomy was performed on day 3 after birth in the NFS/*sld* mice (22). A total of 35 NFS/*sld* mice that had been subjected to thymectomy on day 3 after birth were investigated in the present study. An additional group of 10 mice not subjected to thymectomy were also investigated. Rebamipide (Otsuka Pharmaceutical, Tokushima, Japan) was prepared as a suspension in 0.5% carboxymethylcellulose (Dai-Ichi Chemical Industries, Tokyo, Japan) in water.

The following experimental groups were studied: a vehicle-treated control group, which received oral administration of vehicle alone (n = 12), and 2 rebamipide-treated groups, which received oral administration of rebamipide at a dose of either 0.3 mg/kg of body weight (n = 12) or 3 mg/kg of body weight (n = 11). Thymectomized NFS/*sld* mice were given daily oral treatment with rebamipide or vehicle, starting from the age of 4 weeks to age 8 weeks. Nonthymectomized mice (n = 10) received oral administration of vehicle alone.

OT-2 mice (C57BL/6-Tg[TcraTcrb]452Cbn/J) were obtained from Dr. J. Sprent (Garvan Institute of Medical Research, Darlinghurst, New South Wales, Australia). These mice (n = 5) were used in the transfer experiment.

All experiments were approved by the Animal Ethics Board of the University of Tokushima.

Histologic assessment. At the end of the treatment period, all organs were removed from the mice, fixed in 4% phosphate buffered formaldehyde (pH 7.2), and prepared for histologic examination. Formalin-fixed tissue sections were stained with hematoxylin and eosin, and 3 pathologists (NI, RA, and YH) independently evaluated the histologic features without knowledge of the condition of each mouse. Histologic changes were scored on a scale of 1–3, where 1 = no change or slight lymphoid cell infiltration (slight), 2 = mild lymphoid cell infiltration (moderate), and 3 = marked lymphoid cell infiltration with tissue destruction (severe). Histologic evaluation was performed in a blinded manner, and 1 tissue section from each salivary and lacrimal gland was evaluated.

TUNEL assay. Apoptotic cells were detected in tissue sections using the in situ TUNEL kit (Wako Pure Chemical, Osaka, Japan), as previously described (23). Briefly, sections were incubated with proteinase K (400 mg/ml) for 5 minutes, and then presoaked for 10 minutes in terminal deoxynucleotidyl transferase (TdT) buffer (0.5 μmoles/liter of cacodylate, 1 mmole/liter of $CoCl_2$, 0.5 μmoles/liter of dithiothreitol, 0.05% bovine serum albumin, 0.15 moles/liter of NaCl). Sections were incubated for 2 hours at 37°C in 25 μl of TdT solution containing 1× terminal transferase buffer, 0.5 nmoles of biotin-labeled dUTP, and 10 units of TdT.

After the TdT reaction, sections were soaked in TdT blocking buffer (300 nmoles/liter of NaCl, 30 mmoles/liter of trisodium citrate-2-hydrate), incubated with horseradish peroxidase (HRP)–conjugated streptavidin for 30 minutes at room temperature, and developed for 10 minutes in phosphate buffered citrate (pH 5.8) containing 0.6 mg/ml of 3,3′-diaminobenzidine tetrahydrochloride dihydrate (DAB). Nuclei were counterstained with methyl green.

Flow cytometric analysis. Surface markers were identified with monoclonal antibodies (mAb) and using an Epics flow cytometer (Beckman Coulter, Miami, FL). Rat mAb against fluorescein isothiocyanate (FITC)–, phycoerythrin (PE)–, or PE-Cy5–conjugated anti-B220, Thy1.2, CD4, and CD8 (eBioscience, San Diego, CA) were used. For detection of T cell activation makers, FITC-conjugated anti-CD25, anti-CD44, anti-CD62L, and anti-CD69 mAb (eBioscience) were used. For detection of B cell surface IgM and IgG1, FITC-conjugated anti-IgM (eBioscience) and anti-IgG1 (BD Phar-

Mingen, San Diego, CA) mAb were used. PE-conjugated anti-Ly5.2 (eBioscience) and biotin-conjugated anti-V_β5.2 and PE-Cy5–conjugated streptavidin (both from BD PharMingen) were used for in vivo ovalbumin-specific T cell expansion. Data were analyzed with FlowJo FACS analysis software (Tree Star, Ashland, OR).

Transfer of OT-2 T cells. Purified CD4+ T cells (5×10^6) derived from the spleen of transgenic OT-2 mice were labeled with carboxyfluorescein succinimidyl ester (CFSE; Molecular Probes, Eugene, OR) and transferred intravenously into B6 (Ly5.1+) mice. One day later, ovalbumin peptide (100 μg) was injected intraperitoneally and rebamipide (0–200 μM; 250 μl per mouse) was injected intravenously into recipient mice. Three days later, cell division was evaluated by flow cytometry to detect the CFSE dilution of the Ly5.2+,V_β5.2+, CD4+ T cells.

Real-time quantitative reverse transcription–polymerase chain reaction analysis. Total RNA was extracted from cultured T cells and B cells derived from the spleen of NFS/*sld* mice with Isogen (Wako Pure Chemical), and reverse transcribed. Transcript levels of NF-κB, FasL, interferon regulatory factor 4 (IRF-4), B lymphocyte–induced maturation protein 1 (BLIMP-1), and β-actin were determined with a PTC-200 DNA Engine Cycler (MJ Research, Waltham, MA) with SYBR Premix Ex Tag (Takara, Kyoto, Japan). The following primer sequences were used: for NF-κB, 5′-ATGGCAGACGATGATCCCTA-3′ (forward) and 5′-TAGGCAAGGTCAGAATGCAC-3′ (reverse); for FasL, 5′-ACTGGACAGATATGGGCCCAC-3′ (forward) and 5′-GCCTCTGTGAGGTAGTAAGTAG-3′ (reverse); for IRF-4, 5′-GAAGCCCCAAAGCCCTCAGTCGTTG-3′ (forward) and 5′-CGCTGAGGAGGAAACTGAA-3′ (reverse); for BLIMP-1, 5′-CATTCCTGTCCCCAACGCATCAACTG-3′ (forward) and 5′-GGTGCCCAAGCACCAAAGTCATAG-3′ (reverse); and for β-actin, 5′-GTGGGCCGCTCTAGGCACCA-3′ (forward) and 5′-CGGTTGGCCTTAGGGTTCAGGGGGG-3′ (reverse). Results were calculated with DNA Engine Opicon System software (Roche Molecular Systems, Alameda, CA).

Western blot analysis. Cell extracts from the nucleus and cytoplasm of T cells and B cells were prepared using a Nuclear/Cytosol Fractionation kit (BioVision, Mountain View, CA). Cells were briefly washed, collected in ice-cold phosphate buffered saline (PBS) in the presence of phosphatase inhibitors, and centrifuged at 500 revolutions per minute for 5 minutes. The pellets were resuspended in a hypotonic buffer, treated with detergent, and centrifuged at 14,000*g* for 30 seconds. The cytoplasmic fraction was collected, the nuclei were lysed, and nuclear proteins were solubilized in lysis buffer containing protease inhibitors. A total of 10 μg of each sample per well was used for sodium dodecyl sulfate–polyacrylamide gel electrophoresis. After blocking with 5% nonfat milk, the membrane was incubated with primary antibodies against phospho-IκBα and NF-κB p65 (RelA) (Santa Cruz Biotechnology, Santa Cruz, CA). Antigen–antibody complexes were detected using a HRP-conjugated secondary antibody. Protein binding was visualized with enhanced chemiluminescence Western blotting reagent (Amersham Biosciences, Arlington Heights, IL). Anti-mouse histone H1 or GAPDH monoclonal antibody (Santa Cruz Biotechnology) was used as the control for protein loading.

Measurement of fluid secretion. Analysis of tear and saliva volumes in rebamipide-treated thymectomized NFS/*sld* mice was performed according to a previously described method (24).

Proliferation assay. CD4+ T cells (1×10^5) purified from spleen cells using anti-B220 mAb, anti-CD8 mAb, and anti-rat IgG conjugated to magnetic beads (Dynal, Oslo, Norway) were placed in RPMI 1640 containing 10% fetal calf serum (FCS), 100 units/ml of penicillin, 0.1 mg/ml of streptomycin, and 50 μM 2-mercaptoethanol and were stimulated with recombinant α-fodrin protein (JS-1) (25) or with plate-coated anti-CD3 and anti-CD28 mAb in 96-well, flat-bottomed plates for 72 hours. Then, ^{3}H-thymidine (1 μCi/well; NEN Life Science Products, Boston, MA) was pulsed into the cell mixture during the final 20 hours of culture. Incorporation of ^{3}H-thymidine was assayed with an automated liquid scintillation counter.

For detection of the proliferation of the CD4+ T cell subset, CFSE-labeled CD4+ T cells were cultured for 72 hours. The CD4+ T cells were then stained with anti-CD4 mAb, and cell division of the CD4+ gated T cells was analyzed by flow cytometer.

Assay of immunoglobulin secretion from B cells. B cells (1×10^5) purified from spleen cells using anti-CD4 mAb, anti-CD8 mAb, and anti-rat IgG conjugated to magnetic beads (Dynal) were placed in RPMI 1640 containing 10% FCS, penicillin/streptomycin, and 2-mercaptoethanol and were stimulated with 10 μg/ml of lipopolysaccharide (LPS; Sigma, St. Louis, MO) and 50 ng/ml of interleukin-4 (IL-4; eBioscience) in 96-well round-bottomed plates for 5 days. Cell surface expression of IgM and IgG1 was detected by flow cytometric analysis, and secreted IgM and IgG1 in the culture supernatants were measured by enzyme-linked immunosorbent assay (ELISA).

Serum autoantibody and cytokine ELISAs. JS-1, SSA/Ro, SSB/La, or single-stranded DNA (ssDNA) antibody was used to coat 96-well plates (24). After the plates were washed, diluted mouse sera were added. HRP-conjugated anti-mouse IgG (heavy and light chains; Vector, Burlingame, CA) was added as the secondary antibody, and *o*-phenylenediamine (OPD; Sigma) buffer was added. Antibodies were measured with an ELISA reader (Model 680; Bio-Rad, Richmond, CA) and with a spectrophotometer at 490 nm.

Serum immunoglobulins were determined by ELISA using a mouse immunoglobulin quantitation kit (Bethyl Laboratories, Montgomery, TX). Briefly, for the IgM and IgA ELISAs, sera were diluted 1:5,000 in PBS, and for the IgG ELISA, sera were diluted 1:25,000 in PBS. Plates were coated with a capture antibody and then washed with PBS–0.1% Tween 20. Diluted sera or culture supernatants were added to the plates and incubated. After washing with PBS–0.1% Tween 20, an HRP-conjugated detection antibody was added. Plates were again washed with PBS–0.1% Tween 20, and OPD buffer was added. Plates were then analyzed with a spectrophotometer at 490 nm, as described previously (26).

Levels of IL-2, interferon-γ (IFNγ), IL-4, and IL-10 in culture supernatants from splenic CD4+ T cells stimulated with anti-CD3 and anti-CD28 for 72 hours were determined by ELISA. Specific antibodies for each cytokine were used in the ELISAs, as previously described (27).

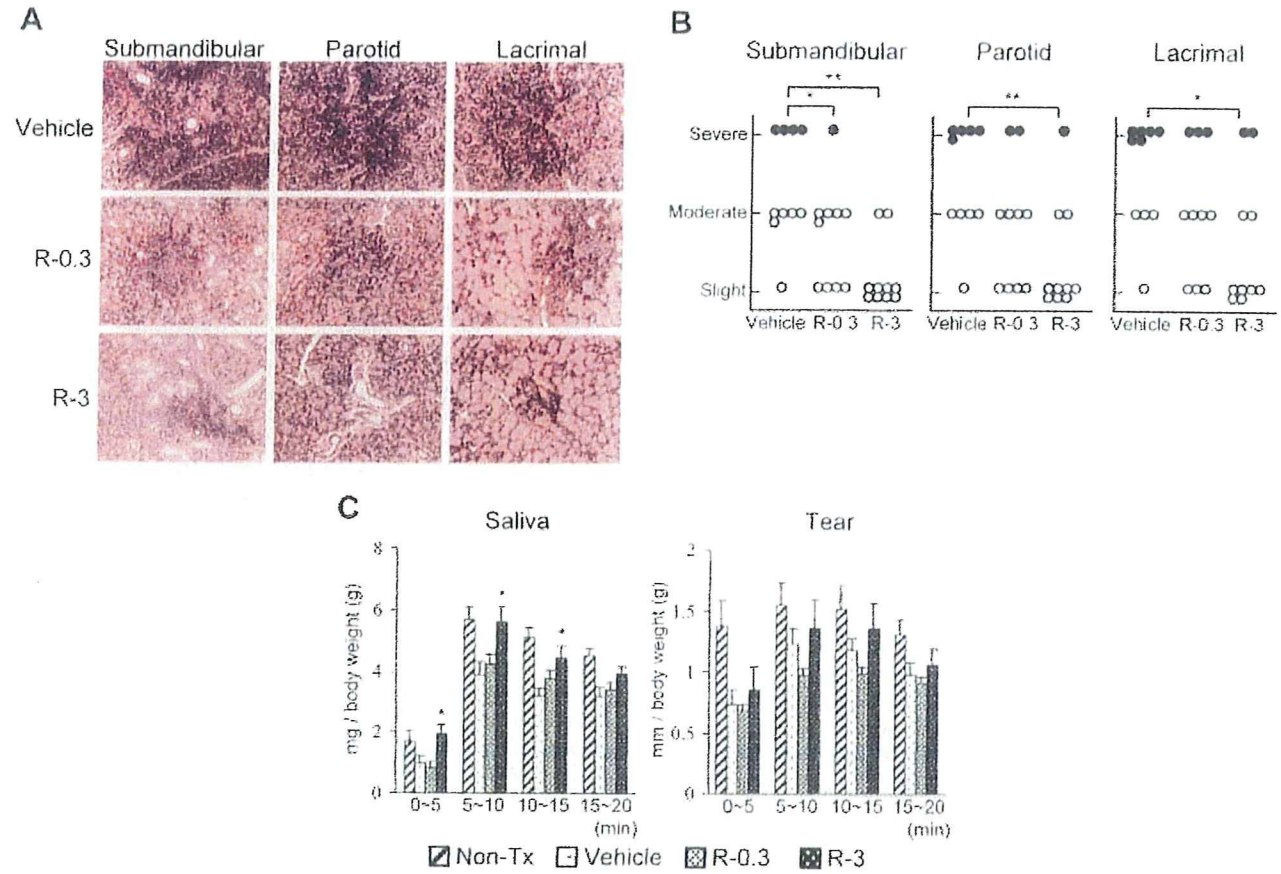

Figure 1. Therapeutic effect of rebamipide on autoimmune lesions in the NFS/*sld* mouse model of Sjögren's syndrome. Mice underwent thymectomy on day 3 after birth and were treated with vehicle, 0.3 mg/kg of rebamipide (R-0.3), or 3 mg/kg of rebamipide (R-3) from age 4 weeks to age 8 weeks. **A,** Sections of salivary and lacrimal glands from the 3 groups of mice. Results are representative of 10 mice per group (hematoxylin and eosin stained; magnification × 100). **B,** Histologic grading of inflammatory lesions in salivary and lacrimal glands from individual mice in the 3 treatment groups. * = $P < 0.05$; ** = $P < 0.01$ by lower-tailed Shirley-Williams test. The mean ± SD histology sores in the vehicle, rebamipide 0.3 mg/kg, and rebamipide 3 mg/kg groups were 2.3 ± 0.7, 1.7 ± 0.7, and 1.2 ± 0.4 for the submandibular glands, 2.4 ± 0.7, 1.8 ± 0.8, and 1.4 ± 0.7 for the parotid glands, and 2.5 ± 0.7, 2.0 ± 0.8, and 1.6 ± 0.8 for the lacrimal glands, respectively. **C,** Average saliva and tear volumes after pilocarpine administration (5 mg/kg) in mice of the 3 treatment groups and in a group of nonthymectomized (non-Tx), vehicle-treated mice at different time periods after pilocarpine administration. Values are the mean and SEM of 10–12 mice per group. * = $P < 0.05$ versus the vehicle-treated control group, by Dunnett's test.

Statistical analysis. Statistical analysis was performed using the Jonckheere trend test and the lower-tailed Shirley-Williams test, Dunnett's test, Student's *t*-test, and chi-square test, as appropriate.

RESULTS

Therapeutic effect of oral administration of rebamipide. In our previous study (22), we found that NFS/*sld* mice subjected to thymectomy on day 3 after birth began to develop autoimmune lesions of the salivary and lacrimal glands at 4 weeks of age or later, while no inflammatory lesions were observed in nonthymectomized NFS/*sld* mice. In the present study, we investigated whether oral administration of rebamipide protects NFS/*sld* mice against the development of autoimmune lesions. To evaluate whether rebamipide treatment was effective at preventing the SS autoimmune pathology, the drug or vehicle alone was administered orally each day to thymectomized NFS/*sld* mice beginning at the age of 4 weeks and continuing to the age of 8 weeks, then organs were removed for histologic analysis.

Salivary and lacrimal glands were stained with hematoxylin and eosin, and histologic features were assessed. Treatment with rebamipide at a concentration of 3 mg/kg prevented the development of autoimmune

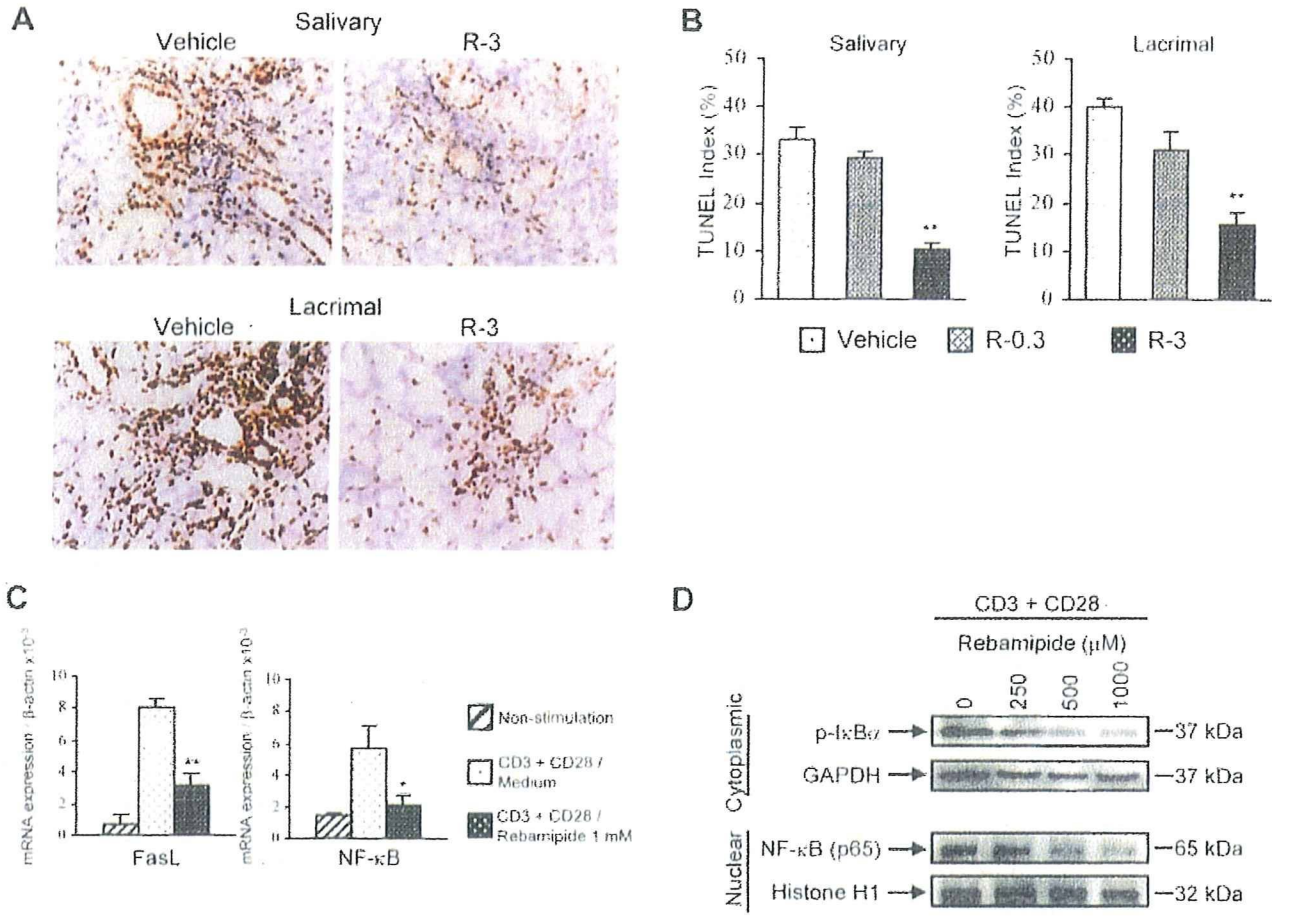

Figure 2. Inhibitory effect of rebamipide on apoptosis of salivary gland cells in the NFS/*sld* mouse model of Sjögren's syndrome. Mice underwent thymectomy on day 3 after birth and were treated with vehicle, 0.3 mg/kg of rebamipide (R-0.3), or 3 mg/kg of rebamipide (R-3) from age 4 weeks to age 8 weeks. **A,** TUNEL assay for apoptotic cells in the salivary and lacrimal glands of mice treated with vehicle or with 3 mg/kg of rebamipide. Results are representative of 5–8 mice per group (magnification × 100). **B,** Percentages of TUNEL+ salivary and lacrimal epithelial cells in the 3 treatment groups. Positive cells were enumerated using a 10 × 20–μm grid net disc covering an objective area of 0.16 mm^2 (n = 10 fields per section). Values are the mean and SEM of 5 mice per group. ** = $P < 0.01$ versus the vehicle-treated group, by Dunnett's test. **C,** Inhibitory effect of rebamipide on T cell activation. Purified CD4+ T cells derived from mouse spleens were stimulated with plate-coated anti-CD3 and anti-CD28 monoclonal antibody for 2 hours in the presence of rebamipide. Levels of mRNA for FasL and NF-κB were detected by quantitative reverse transcription–polymerase chain reaction analysis. Values are the mean and SEM expression relative to β-actin mRNA in triplicate wells. * = $P < 0.01$; ** = $P < 0.05$ versus medium containing anti-CD3 and anti-CD28, by Student's *t*-test. **D,** Phosphorylation of IκB and nuclear translocation of NF-κB in cytoplasmic and nuclear extracts of activated CD4+ T cells treated with CD3 and CD28 ligation in the presence of rebamipide, as analyzed by Western blotting. GAPDH and histone H1 were used as the respective internal controls. Results are representative of 3 independent experiments.

lesions in the submandibular ($P < 0.01$), parotid ($P < 0.01$), and lacrimal ($P < 0.05$) glands (Figures 1A and B). Rebamipide treatment at a concentration of 0.3 mg/kg prevented the development of autoimmune lesions in the submandibular glands alone ($P < 0.05$). Mononuclear cell infiltration as well as destruction of the parenchyma was inhibited in the salivary and lacrimal glands of thymectomized NFS/*sld* mice treated with rebamipide. The average saliva volume, but not tear volume, in the rebamipide-treated group was significantly higher than that in the vehicle-treated control group (Figure 1C).

We previously demonstrated that epithelial cell apoptosis via the Fas/FasL system plays an important role in the development of autoimmune lesions in this mouse model of SS, and a significant increase in TUNEL+ apoptotic epithelial duct cells in the salivary glands was detected in this mouse model (11). In the

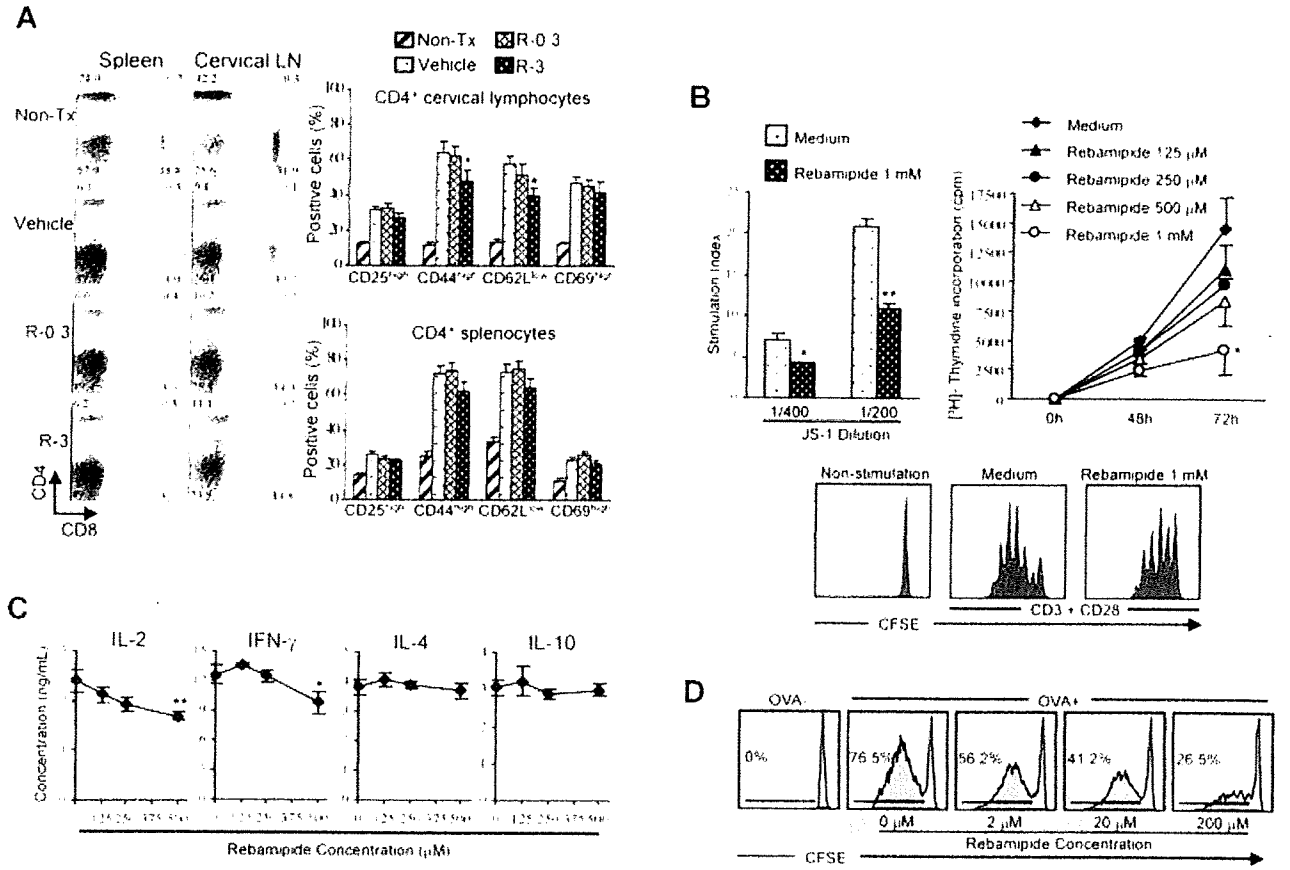

Figure 3. Effect of rebamipide on T cell phenotypes and functions in the NFS/*sld* mouse model of Sjögren's syndrome. Mice underwent thymectomy on day 3 after birth and were treated with vehicle, 0.3 mg/kg of rebamipide (R-0.3), or 3 mg/kg of rebamipide (R-3) from age 4 weeks to age 8 weeks. A group of nonthymectomized (non-Tx), vehicle-treated mice was also studied. **A,** CD4+ and CD8+ T cell subsets in the spleen and cervical lymph nodes of the 4 groups of mice, as analyzed by flow cytometry (left). Numbers shown in each compartment are the percentage of positive cells. Results are representative of 10 mice per group. Memory markers on CD4+ T cells derived from the cervical lymph nodes and spleen of the 4 groups of mice were also analyzed by flow cytometry (right). Values are the mean and SEM of 10 mice per group. **B,** Antigen-specific and nonspecific T cell responses. Purified CD4+ T cells from the spleen of thymectomized mice were cultured for 72 hours with irradiated T cell–depleted splenocytes in the presence of recombinant α-fodrin (JS-1), with and without rebamipide (top left). Values are the mean and SEM. * = $P < 0.05$; ** = $P < 0.01$ versus medium alone, by Dunnett's test. Incorporation of ^{3}H-thymidine into purified CD4+ T cells stimulated with anti-CD3 and anti-CD28 monoclonal antibodies (mAb) and treated for 48 or 72 hours with the indicated concentrations of rebamipide or medium alone was determined during the last 12 hours of culture (top right). Results are representative of 3 independent experiments. Values are the mean and SEM of triplicate wells. In addition, CD4+ T cells were labeled with carboxyfluorescein succinimidyl ester (CFSE) and were left unstimulated or were stimulated with anti-CD3 and anti-CD28 mAb for 72 hours in the presence of medium alone or 1 m*M* rebamipide (bottom). Cell division was analyzed by flow cytometry. * = $P < 0.01$ versus medium alone, by Dunnett's test. **C,** Production of interleukin-2 (IL-2), interferon-γ (IFNγ), IL-4, and IL-10 by CD4+ T cells stimulated for 72 hours with anti-CD3 and anti-CD28 mAb in the presence of medium alone or the indicated concentrations of rebamipide, as determined by enzyme-linked immunosorbent assay of culture supernatants. Results are representative of 3 independent experiments. Values are the mean ± SEM of triplicate samples. * = $P < 0.05$; ** = $P < 0.01$ versus medium alone, by Dunnett's test. **D,** Flow cytometry of CFSE-labeled CD4+ T cells (5×10^6) derived from transgenic OT-2 mice and transferred intravenously into B6 (Ly5.1+) mice. Ovalbumin (OVA) peptide (100 μg) was injected intraperitoneally, and rebamipide (0–200 μ*M*) was injected intravenously, into recipient mice. After 3 days, the CFSE dilution of Ly5.2+,V_β5.2+,CD4+ T cells was analyzed. Results are representative of 3–5 mice per group.

present study, we observed a decrease in TUNEL+ apoptotic epithelial cells in the salivary glands of mice treated with rebamipide as compared with those in vehicle-treated mice (Figures 2A and B). Indeed, expression of FasL and NF-κB genes on CD4+ T cells was significantly inhibited by rebamipide treatment (Figure 2C), possibly being consistent with the finding of decreased TUNEL+ epithelial cell apoptosis in the

Table 1. Autoantibody production in the NFS/*sld* mouse model of Sjögren's syndrome after treatment with rebamipide or vehicle alone*

Antibody	No. (%) of nonthymectomized, vehicle-treated mice (n = 10)	Treatment in thymectomized mice		
		No. (%) receiving vehicle (n = 12)	No. (%) receiving 0.3 mg/kg of rebamipide (n = 12)	No. (%) receiving 3 mg/kg of rebamipide (n = 11)
SSA/Ro	0 (0)	12 (100)	11 (92)	8 (73)†
SSB/La	0 (0)	11 (92)	10 (83)	6 (55)†
JS-1	0 (0)	7 (58)	4 (33)	4 (36)
ssDNA	0 (0)	11 (92)	12 (100)	7 (64)

* Mice were subjected to thymectomy on day 3 after birth. Autoantibodies were detected by enzyme-linked immunosorbent assay of sera obtained at the end of treatment (8 weeks of age). A positive result was defined as a value higher than the mean ± 3SD of the optical density value in nonthymectomized NFS/*sld* mice. JS-1 is an α-fodrin–specific antibody. ssDNA = single-stranded DNA.
† $P < 0.05$ versus vehicle-treated mice, by chi-square test.

rebamipide-treated mice. In addition, we confirmed the dose-dependent decrease in phosphorylation of IκB in CD4+ T cells from mice treated with rebamipide as compared with vehicle-treated controls (Figure 2D). Furthermore, nuclear translocation of NF-κB subunits (RelA and p65) in CD4+ T cells from rebamipide-treated mice had decreased remarkably compared with that in cells from vehicle-treated controls (Figure 2D).

Inhibitory effects of rebamipide on T cell activation. We next examined whether the therapeutic effect of oral administration of rebamipide on thymectomized NFS/*sld* mice was attributable to the inhibition of T cell activation. Cervical lymph node cells and spleen cells were purified from thymectomized NFS/*sld* mice treated with rebamipide or vehicle from ages 4 weeks to 8 weeks. In rebamipide-treated mice, the number of CD4+ and CD8+ T cells from the lymph node and spleen did not change with oral administration of rebamipide at either dose (Figure 3A).

We next examined CD25, CD44, CD62L, and CD69 expression on CD4+ T cells because these makers are known to be highly expressed on activated T cells and memory T cells (28). We found a decreased expression of CD4+,CD62L^{low} effector T cells in lymph nodes from mice treated with rebamipide, as compared with those from the control group (Figure 3A). In contrast, the expression of these markers on splenic CD4+ T cells from rebamipide-treated mice was similar to that in splenic CD4+ T cells from vehicle-treated controls (Figure 3A). It has recently been demonstrated that autoimmunity could be induced by specific in vivo expansion of CD4+,CD62L^{low} effector T cells (29).

Inhibitory effects of rebamipide on T cell proliferation and cytokine production. We previously reported that CD4+ T cells from thymectomized mice responded to the α-fodrin peptide JS-1 (25). Thus, we examined whether the rebamipide treatment affects the JS-1–specific proliferative response of splenic CD4+ T cells. A significant decrease in autoantigen (JS-1)–specific T cell proliferation was observed in CD4+ T cells treated with rebamipide (Figure 3B, top left). These results suggest that rebamipide treatment reduced the expansion of JS-1–specific T cells in mice, which is consistent with the low levels of CD4+,CD62L^{low} effector T cells in the rebamipide-treated mice. The proliferative response of anti-CD3 and anti-CD28 mAb-stimulated CD4+ T cells was also decreased by the addition of rebamipide in a dose-dependent manner (Figure 3B, top right). Furthermore, when CFSE-labeled CD4+ T cells were stimulated with anti-CD3 and anti-CD28 mAb in the presence of rebamipide for 72 hours, cell division was suppressed by rebamipide (Figure 3B, bottom).

To confirm the inhibitory effect of rebamipide, an in vitro cytokine assay was performed using splenic CD4+ T cells stimulated with anti-CD3 and anti-CD28. We obtained clear evidence that rebamipide treatment inhibited the production of Th1 (IL-2 and IFNγ), but not Th2 (IL-4 and IL-10), cytokines (Figure 3C). In serum samples, we detected no IL-2, IL-4, or IFNγ in mice treated with rebamipide (data not shown).

It was still unclear whether the antigen-specific T cell response in a normal mouse strain is inhibited by rebamipide. Therefore, CFSE-labeled T cells from OT-2 mice transgenic for ovalbumin-specific T cell receptor

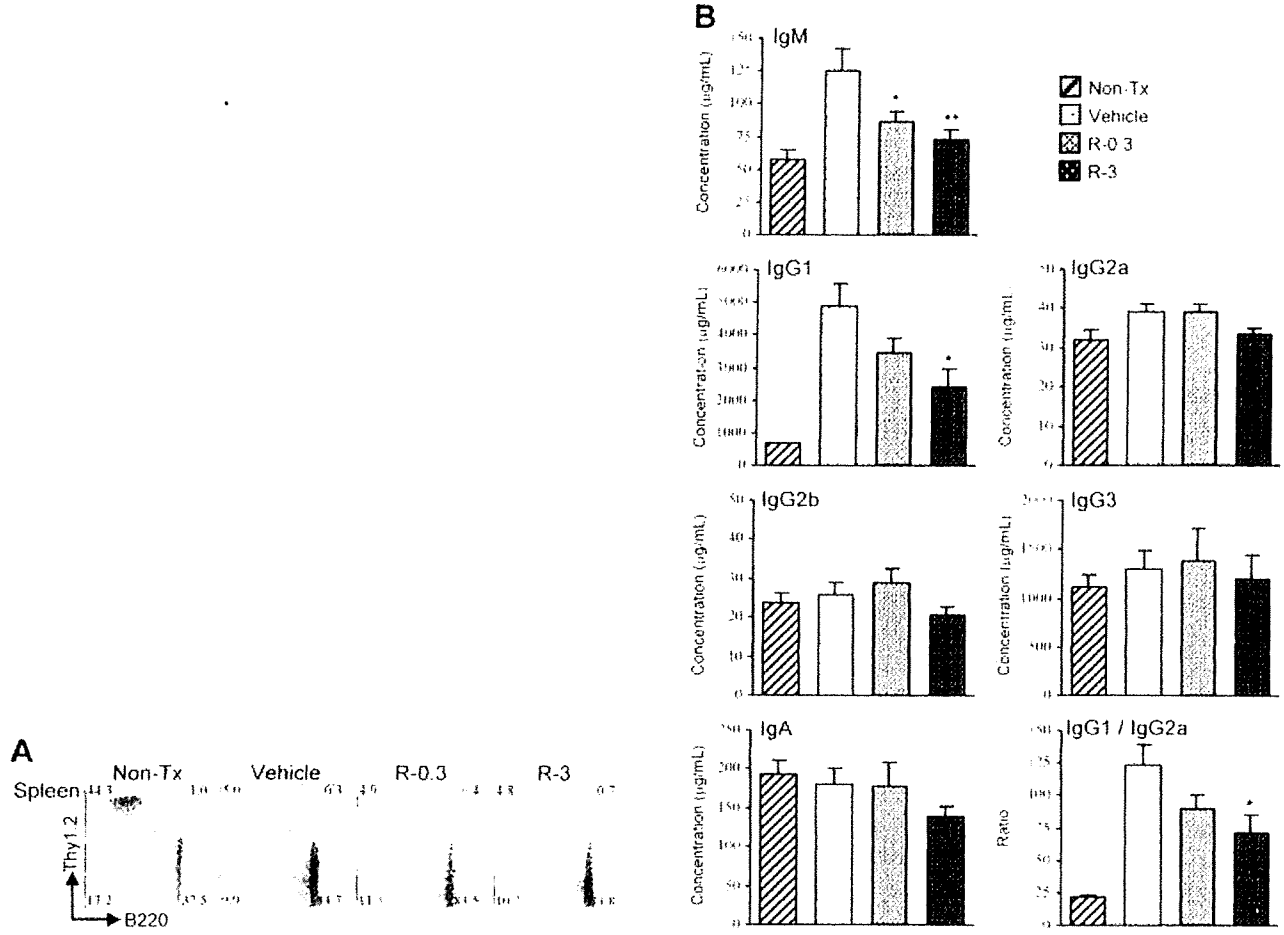

Figure 4. Effect of rebamipide on B cell function in the NFS/*sld* mouse model of Sjögren's syndrome after treatment with rebamipide. Mice underwent thymectomy on day 3 after birth and were treated with vehicle, 0.3 mg/kg of rebamipide (R-0.3), or 3 mg/kg of rebamipide (R-3) from age 4 weeks to age 8 weeks. A group of nonthymectomized (non-Tx), vehicle-treated mice was also studied. **A,** Thy1.2+ and B220+ cell subsets in the spleen of the 4 groups of mice, as determined by flow cytometry. Numbers shown in each compartment are the percentage of positive cells. Results are representative of 10–12 mice per group. **B,** Serum concentrations of immunoglobulin subclasses in the 4 groups of mice, as determined by enzyme-linked immunosorbent assay. Values are the mean and SEM of 10 mice per group. * = $P < 0.05$; ** = $P < 0.01$ versus the vehicle-treated group, by Dunnett's test.

were transferred into B6 (Ly5.1+) mice, and ovalbumin peptide was injected into the mice together with rebamipide. Treatment with rebamipide resulted in a dose-dependent inhibition of ovalbumin-specific T cell expansion in vivo (Figure 3D).

Reduced serum autoantibody production with rebamipide treatment. Sera were collected after rebamipide and vehicle treatment to evaluate the production of autoantibodies. Thymectomized NFS/*sld* mice have high titers of serum autoantibody against recombinant α-fodrin protein (JS-1) (25). We examined whether oral administration of rebamipide affected serum levels of autoantibody against α-fodrin in this mouse model of SS. As shown in Table 1, the titer of autoantibody against α-fodrin (JS-1) was considerably lower in mice treated with rebamipide than in mice treated with vehicle. The decreased serum titer of autoantibody against α-fodrin suggests that oral administration of rebamipide affected the autoimmune pathology and was able to suppress the systemic production of α-fodrin–specific autoantibody. We also examined serum titers of autoantibodies that are often associated with SS: anti-SSA/Ro, anti-SSB/La, anti-ssDNA, and anti–α-fodrin (30–33). Serum titers of anti-SSA/Ro and anti-SSB/La autoantibodies were significantly decreased in mice treated with rebamipide, but titers of anti–α-fodrin were not statistically significantly different from those in the control mice (Table 1).

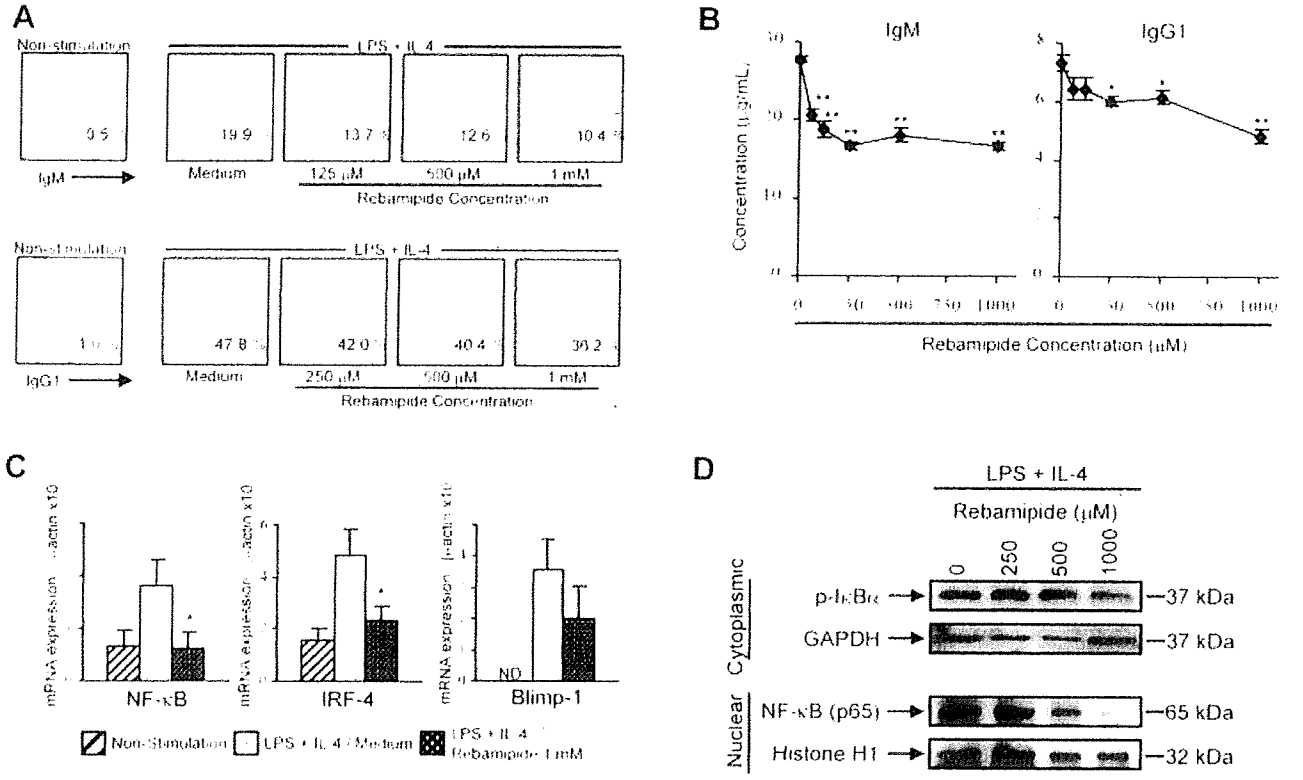

Figure 5. Effect of rebamipide on immunoglobulin production in the NFS/*sld* mouse model of Sjögren's syndrome. Mice underwent thymectomy on day 3 after birth and were treated with 3 mg/kg of rebamipide from age 4 weeks to age 8 weeks. **A,** Cell surface expression of IgM and IgG1, as detected by flow cytometry. Enriched splenic B cells were left unstimulated or were stimulated with lipopolysaccharide (LPS) and interleukin-4 (IL-4) in the presence of the indicated concentrations of rebamipide for 5 days. Values are the percentage of positive cells. **B,** Secretion of IgM and IgG1 into supernatants from B cells stimulated for 5 days with LPS and IL-4 in the presence of the indicated concentrations of rebamipide, as detected by enzyme-linked immunosorbent assay. Values are the mean ± SEM of 10 mice. * = $P < 0.05$; ** = $P < 0.01$ versus medium alone, by Dunnett's test. **C,** Expression of mRNA for NF-κB, interferon regulatory factor 4 (IRF-4), and B lymphocyte–induced maturation protein 1 (BLIMP-1), by stimulated B cells, as determined by quantitative reverse transcription–polymerase chain reaction analysis. Results are representative of 3 independent experiments. Values are the mean and SEM expression relative to β-actin mRNA in triplicate wells. * = $P < 0.05$ versus medium alone, by Student's *t*-test. ND = not detected. **D,** Phosphorylation of IκB and nuclear translocation of NF-κB in cytoplasmic and nuclear extracts of activated B cells treated with LPS and IL-4 in the presence of rebamipide, as analyzed by Western blotting. GAPDH and histone H1 were use as the respective internal controls. Results are representative of 3 independent experiments.

Reduced serum immunoglobulin levels with rebamipide treatment. In rebamipide-treated mice, the number of splenic B220+ B cells did not change with oral administration of either dose of rebamipide (Figure 4A). We found that thymectomized NFS/*sld* mice developed hypergammaglobulinemia involving both IgG1 and IgM as compared with nonthymectomized control mice (Figure 4B). Rebamipide-treated mice showed prominent inhibition of serum IgM and IgG1 levels ($P < 0.01$), but not the other IgG subclasses or IgA (Figure 4B). This may indicate that oral administration of rebamipide affected all B cell function, which was able to suppress systemic secretion of IgM and IgG1.

Inhibitory effects of rebamipide on immunoglobulin secretion. To confirm the inhibitory effects of rebamipide on IgM and IgG1 secretion, we examined the effects of in vitro treatment with rebamipide using splenic B220+ B cells stimulated with LPS and IL-4. We found that rebamipide inhibited B cell production of IgM and IgG1, as determined by flow cytometry (Figure 5A). Rebamipide also inhibited IgM and IgG1 in culture supernatants, as determined by ELISA (Figure 5B). Both of these effects were dose-dependent. Since rebamipide treatment in this mouse model of SS inhibited the production of autoantibodies and immunoglobulins, we also examined the transcriptional activity of NF-κB,

IRF-4, and BLIMP-1. Significant inhibitory effects of rebamipide on the expression of mRNA for NF-κB and IRF-4, transcription factors that are associated with B cell activation and differentiation, were observed (Figure 5C). We confirmed the dose-dependent decrease in phospho-IκB and NF-κB subunits (p65) in activated B cells stimulated with LPS and IL-4 as compared with vehicle-treated controls (Figure 5D).

DISCUSSION

Since studies of animal models of autoimmune disorders should eventually give rise to appropriate potential treatments in humans with those diseases, it is important to identify the best therapeutic approach by which cells of the immune system can be specifically affected without causing side effects. In this regard, antigen-specific down-regulation of autoimmune processes is considered to be the most suitable therapy (34–36). The findings of the present study of rebamipide treatment in the NFS/*sld* mouse model of Sjögren's syndrome confirm the protective effect of rebamipide on the functional recovery of T cells and B cells in this autoimmune exocrinopathy, probably based on its capacity to inhibit T cell activation and B cell proliferation, in addition to reinforcing the epithelial barrier. Although therapy in SS patients has generally consisted of systemic administration of immunosuppressive or antimuscarinic drugs, it has been known that the systemic use of these drugs induces severe side effects (34). In contrast, it has been reported that oral administration of rebamipide had no clinically significant physical side effects, with normal blood pressure and pulse rate, in healthy adult subjects (37). This study is the first to demonstrate that oral administration of rebamipide effectively inhibits autoimmune pathology in the NFS/*sld* mouse model of SS without causing systemic histopathologic changes.

We previously reported that a cleavage product of 120-kd α-fodrin may be an important autoantigen in the development of primary SS and that anti–120-kd α-fodrin antibodies have been frequently detected in sera from SS patients (25). We have also reported a significant increase in TUNEL+ apoptotic epithelial duct cells in the salivary glands of thymectomized NFS/*sld* mice and a large proportion of FasL in tissue-infiltrating CD4+ T cells (11); both findings support the idea that tissue-infiltrating CD4+ T cells are responsible for tissue destruction, as determined by in vitro cytotoxicity assay. Our data have suggested that one mechanism by which activated CD4+ T cells induce cytotoxicity to salivary gland cells in this murine model of SS is Fas-based and that the primary mediators of the disease are autoantigen-driven T cell responses. In the present study, we found that expression of FasL on CD4+ T cells was significantly inhibited and that TUNEL+ epithelial cell apoptosis declined in the rebamipide-treated mice. A significant decrease in autoantigen-specific T cell proliferation was observed in CD4+ T cells with rebamipide treatment. This is consistent with the finding that rebamipide treatment resulted in the dose-dependent inhibition of ovalbumin-specific T cell expansion in vivo.

In addition, we observed that rebamipide treatment induced a selective impairment of CD4+,CD62L^{low} effector T cells in the lymph nodes. This population was more potent than the population of CD4+,CD62L^{high} cells in inducing a self-directed immune response, as demonstrated by cytometric isolation and adoptive transfer experiments. The induction of autoimmunity by specific in vivo expansion of CD4+,CD62L^{low} cells has recently been demonstrated (29), indicating that CD4+,CD62L^{low} effector T cells may be attractive targets for immune interventions in the treatment of autoimmune diseases. On the other hand, rebamipide treatment did not influence the frequency of CD4+,CD25+ natural regulatory T cells in cervical lymph nodes (data not shown). It is noteworthy that rebamipide treatment inhibited T cell proliferation and Th1 cytokine production (IL-2 and IFNγ). These data indicate that rebamipide treatment effectively inhibits autoimmune pathology in the NFS/*sld* mouse model of SS.

The improvement in secretory function after treatment with rebamipide, as demonstrated by saliva volumes, strongly points to the ingestive mechanism of action of rebamipide. With regard to the small discrepancy between the histologic features of the lacrimal glands and the lacrimal gland function, as demonstrated by tear flow volumes after treatment of rebamipide (see Figure 1), it has been reported that inflammatory lesions in the lacrimal gland develop later than those in the salivary gland in our mouse model (22). It is also possible that the effects of rebamipide on salivary gland cells may be different from the effects on lacrimal gland cells.

The beneficial effects of rebamipide on the epithelial barrier, which have previously been demonstrated in the gastric and small intestinal mucosa (38,39), have possibly, although not definitively, also been shown for the salivary gland epithelia, although the findings are not definitive. While the mechanism of action of rebamipide

on epithelial permeability, which has mostly been studied in the stomach, is not completely understood, it could be related to the capacity of rebamipide to act as a scavenger of cytokine-induced hydroxyl radicals (40) or to induce prostaglandin production (41). Since we found decreased apoptosis of salivary gland epithelia in rebamipide-treated mice, it is possible that the protective effect of rebamipide on the salivary gland epithelia could also account for its beneficial effect on ulcerative colitis in humans or on Dextran sulfate sodium–induced colitis in rats (42). This improvement in the epithelial barrier, together with the capacity of rebamipide to modulate immune responses, may represent a new therapeutic approach to the clinical management of sicca syndrome in SS patients without producing any side effects.

Rebamipide treatment clearly inhibited the production of serum autoantibodies, IgM, and IgG1 and induced a reduction in the transcriptional activity of IRF-4 via down-regulation of NF-κB. It has been reported that IRF-4 functions redundantly with IRF-8 to regulate B cell differentiation into immature IgM+ B cells (43). IRF-4 has been shown to regulate the induction of BLIMP-1 expression and BLIMP-1–dependent plasma cell differentiation (44). The majority of IgM and IgG1 are autoreactive and are also reactive with DNA, phosphorylcholine, phosphatidylcholine, and α1–3-dextran. The process of autoantibody production in SS is characterized by findings of both an antigen-driven response and a polyclonal B cell activation. The causes of this abnormal activation have not been fully elucidated and are likely to vary in different patients and in different animal models of autoimmune diseases. These diseases are characterized by a high titer of autoantibodies that may play a role in the tissue damage. It is possible that the down-regulatory effect of rebamipide on the immune response would be a good therapeutic approach.

We have previously reported that treatment with anti-CD4 and anti-CD86 mAb, cathepsin S inhibitor, caspase inhibitor, and cyclosporin A improved the autoimmune pathology in this mouse model of SS (11,45–48). In the present study, we observed less drastic effects of rebamipide on histologic features, as compared with those in previous therapeutic experiments. This may be related to the relatively low degree of inhibitory effects on T cell–mediated immune responses. Although we did not simply compare the efficacy of rebamipide with that of systemic administration of a different agent, this successful therapeutic effect of rebamipide would provide the possibility of establishing a new form of therapy for patients with autoimmune symptoms caused by SS as well as other types of diseases.

ACKNOWLEDGMENTS

The authors thank Ai Nagaoka, Hiroyo Amo, and Satoko Yoshida for technical assistance.

AUTHOR CONTRIBUTIONS

Dr. Hayashi had full access to all of the data in the study and takes responsibility for the integrity of the data and the accuracy of the data analysis.

Study design. Kohashi, Ishimaru, Hayashi.
Acquisition of data. Kohashi, Arakaki.
Analysis and interpretation of data. Kohashi.
Manuscript preparation. Kohashi, Ishimaru, Hayashi.
Statistical analysis. Kohashi.

REFERENCES

1. Fox RI. Sjögren's syndrome. Lancet 2005;366:321–31.
2. Fox RI, Stern M, Michelson P. Update in Sjögren syndrome. Curr Opin Rheumatol 2000;12:391–8.
3. Kruize AA, Smeenk RJ, Kater L. Diagnostic criteria and immunopathogenesis of Sjögren's syndrome: implications for therapy. Immunol Today 1995;16:557–9.
4. Sebzda E, Mariathasan S, Ohteki T, Jones R, Bachmann MF, Ohashi PS. Selection of the T cell repertoire. Annu Rev Immunol 1999;17:829–74.
5. Starr TK, Jameson SC, Hogquist KA. Positive and negative selection of T cells. Annu Rev Immunol 2003;21:139–76.
6. Wakeland EK, Liu K, Graham RR, Behrens TW. Delineating the genetic basis of systemic lupus erythematosus. Immunity 2001;15:397–408.
7. Yasutomo K. Pathological lymphocyte activation by defective clearance of self-ligands in systemic lupus erythematosus. Rheumatology (Oxford) 2003;42:214–22.
8. Marrack P, Kappler J, Kotzin BL. Autoimmune disease: why and where it occurs. Nat Med 2001;7:899–905.
9. Davidson A, Diamond B. Autoimmune diseases. N Engl J Med 2001;345:340–50.
10. Yasutomo K, Horiuchi T, Kagami S, Tsukamoto H, Hashimura C, Urushihara M, et al. Mutation of DNASE1 in people with systemic lupus erythematosus. Nat Genet 2001;28:313–4.
11. Saegusa K, Ishimaru N, Yanagi K, Mishima K, Arakaki R, Suda T, et al. Prevention and induction of autoimmune exocrinopathy is dependent on pathogenic autoantigen cleavage in murine Sjögren's syndrome. J Immunol 2002;169:1050–7.
12. Bieganowska KD, Ausubel LJ, Modabber Y, Slovik E, Messersmith W, Hafler DA. Direct ex vivo analysis of activated, Fas-sensitive autoreactive T cells in human autoimmune disease. J Exp Med 1997;185:1585–94.
13. Miranda-Carus ME, Askanase AD, Clancy RM, Di Donato F, Chou TM, Libera MR, et al. Anti-SSA/Ro and anti-SSB/La autoantibodies bind the surface of apoptotic fetal cardiocytes and promote secretion of TNF-α by macrophages. J Immunol 2000;165:5345–51.
14. Avrameas S. Natural autoantibodies: from 'horror autotoxicus' to 'gnothi seauton'. Immunol Today 1991;12:154–9.
15. Toubi E, Etzioni A. Intravenous immunoglobulin in immunodeficiency states: state of the art. Clin Rev Allergy Immunol 2005;29:167–72.
16. Barabas AZ, Cole CD, Barabas AD, Lafreniere R. Production of

a new model of slowly progressive Heymann nephritis. Int J Exp Pathol 2003;84:245–58.
17. Ravetch JV. Fc Receptors. In: Paul WE, editor. Fundamental immunology. 5th ed. Philadelphia: Lippincott Williams & Wilkins; 2003. p. 685–700.
18. McCarthy J, O'Mahony L, O'Callaghan L, Sheil B, Vaughan EE, Fitzsimons N, et al. Double blind, placebo controlled trial of two probiotic strains in interleukin 10 knockout mice and mechanistic link with cytokine balance. Gut 2003;52:975–80.
19. Kishimoto S, Haruma K, Tari A, Sakurai K, Nakano M, Nakagawa Y. Rebamipide, an antiulcer drug, prevents DSS-induced colitis formation in rats. Dig Dis Sci 2000;45:1608–16.
20. Bamba H, Ota S, Kato A, Miyatani H, Kawamoto C, Yoshida Y, et al. Effect of rebamipide on prostaglandin receptors-mediated increase of inflammatory cytokine production by macrophages. Aliment Pharmacol Ther 2003;18 Suppl 1:113–8.
21. Hayashi Y, Kojima A, Hata M, Hirokawa K. A new mutation involving the sublingual gland in NFS/N mice: partially arrested mucous cell differentiation. Am J Pathol 1988;132:187–91.
22. Haneji N, Hamano H, Yanagi K, Hayashi Y. A new animal model for primary Sjögren's syndrome in NFS/sld mutant mice. J Immunol 1994;153:2769–77.
23. Ishimaru N, Saegusa K, Yanagi K, Haneji N, Saito I, Hayashi Y. Estrogen deficiency accelerates autoimmune exocrinopathy in murine Sjögren's syndrome through Fas-mediated apoptosis. Am J Pathol 1999;155:173–81.
24. Saito I, Haruta K, Shimuta M, Inoue H, Sakurai H, Yamada K, et al. Fas ligand-mediated exocrinopathy resembling Sjögren's syndrome in mice transgenic for IL-10. J Immunol 1999;162:2488–94.
25. Haneji N, Nakamura T, Takio K, Yanagi K, Higashiyama H, Saito I, et al. Identification of α-fodrin as a candidate autoantigen in primary Sjögren's syndrome. Science 1997;276:604–7.
26. Angelin-Duclos C, Johnson K, Liao J, Lin KI, Calame K. An interfering form of Blimp-1 increases IgM secreting plasma cells and blocks maturation of peripheral B cells. Eur J Immunol 2002;32:3765–75.
27. Dong L, Ito S, Ishii KJ, Klinman DM. Suppressive oligodeoxynucleotides delay the onset of glomerulonephritis and prolong survival in lupus-prone NZB × NZW mice. Arthritis Rheum 2005; 52:651–8.
28. Anderson BE, McNiff J, Yan J, Doyle H, Mamula M, Shlomchik MJ, et al. Memory $CD4^+$ T cells do not induce graft-versus-host disease. J Clin Invest 2003;112:101–8.
29. Amend B, Doster H, Lange C, Dubois E, Kalbacher H, Melms A, et al. Induction of autoimmunity by expansion of autoreactive $CD4^+CD62L^{low}$ cells in vivo. J Immunol 2006;177:4384–90.
30. Franceschini F, Cavazzana I. Anti-Ro/SSA and La/SSB antibodies. Autoimmunity 2005;38:55–63.
31. Hayashi Y, Arakaki R, Ishimaru N. Apoptosis and estrogen deficiency in primary Sjögren syndrome [published erratum appears in Curr Opin Rheumatol 2004;16:753]. Curr Opin Rheumatol 2004;16:522–6.
32. Turkcapar N, Olmez U, Tutkak H, Duman M. The importance of α-fodrin antibodies in the diagnosis of Sjögren's syndrome. Rheumatol Int 2006;26:354–9.
33. Chan EK, Hamel JC, Buyon JP, Tan EM. Molecular definition and sequence motifs of the 52-kD component of human SS-A/Ro autoantigen. J Clin Invest 1991;87:68–76.
34. Nepom GT. Therapy of autoimmune diseases: clinical trials and new biologics. Curr Opin Immunol 2002;14:812–5.
35. Peakman M, Dayan CM. Antigen-specific immunotherapy for autoimmune disease: fighting fire with fire? Immunology 2001; 104:361–6.
36. Fox RI, Maruyama T. Pathogenesis and treatment of Sjögren's syndrome. Curr Opin Rheumatol 1997;9:393–9.
37. Hasegawa S, Sekino H, Matsuoka O, Saito K, Sekino H, Morikawa A, et al. Bioequivalence of rebamipide granules and tablets in healthy adult male volunteers. Clin Drug Investig 2003;23:771–9.
38. Matysiak-Budnik T, de Mascarel A, Abely M, Mayo K, Heyman M, Megraud F. Positive effect of rebamipide on gastric permeability in mice after eradication of Helicobacter felis. Scand J Gastroenterol 2000;35:470–5.
39. Matysiak-Budnik T, van Niel G, Megraud F, Mayo K, Bevilacqua C, Gaboriau-Routhiau V, et al. Gastric Helicobacter infection inhibits development of oral tolerance to food antigens in mice. Infect Immun 2003;71:5219–24.
40. Naito Y, Yoshikawa T, Tanigawa T, Sakurai K, Yamasaki K, Uchida M, et al. Hydroxyl radical scavenging by rebamipide and related compounds: electron paramagnetic resonance study. Free Radic Biol Med 1995;18:117–23.
41. Yamasaki K, Kanbe T, Chijiwa T, Ishiyama H, Morita S. Gastric mucosal protection by OPC-12759, a novel antiulcer compound, in the rat. Eur J Pharmacol 1987;142:23–9.
42. Makiyama K, Takeshima F, Kawasaki H, Zea-Iriarte WL. Anti-inflammatory effect of rebamipide enema on proctitis type ulcerative colitis: a novel therapeutic alternative. Am J Gastroenterol 2000;95:1838–9.
43. Lu R, Medina KL, Lancki DW, Singh H. IRF-4,8 orchestrate the pre-B-to-B transition in lymphocyte development. Genes Dev 2003;17:1703–8.
44. Klein U, Casola S, Cattoretti G, Shen Q, Lia M, Mo T, et al. Transcription factor IRF4 controls plasma cell differentiation and class-switch recombination. Nat Immunol 2006;7:773–82.
45. Saegusa K, Ishimaru N, Yanagi K, Haneji N, Nishino M, Azuma M, et al. Treatment with anti-CD86 costimulatory molecule prevents the autoimmune lesions in murine Sjögren's syndrome (SS) through up-regulated Th2 response. Clin Exp Immunol 2000;119: 354–60.
46. Hayashi Y, Ishimaru N, Arakaki R, Tsukumo S, Fukui H, Kishihara K, et al. Effective treatment of a mouse model of Sjögren's syndrome with eyedrop administration of anti-CD4 monoclonal antibody. Arthritis Rheum 2004;50:2903–10.
47. Tsubota K, Saito I, Ishimaru N, Hayashi Y. Use of topical cyclosporin A in a primary Sjögren's syndrome mouse model. Invest Ophthalmol Vis Sci 1998;39:1551–9.
48. Saegusa K, Ishimaru N, Yanagi K, Arakaki R, Ogawa K, Saito I, et al. Cathepsin S inhibitor prevents autoantigen presentation and autoimmunity. J Clin Invest 2002;110:361–9.